SUPERSYMMETRY, PART II (EXPERIMENT)

Updated September 2015 by O. Buchmueller (Imperial College London) and P. de Jong (Nikhef and University of Amsterdam).

II.1. Introduction

Supersymmetry (SUSY), a transformation relating fermions to bosons and vice versa [1–9], is one of the most compelling possible extensions of the Standard Model of particle physics (SM) that could be discovered at high-energy colliders such as the Large Hadron Collider (LHC) at CERN.

On theoretical grounds SUSY is motivated as a generalization of space-time symmetries. A low-energy realization of SUSY, *i.e.*, SUSY at the TeV scale, is, however, not a necessary consequence. Instead, low-energy SUSY is motivated by the possible cancellation of quadratic divergences in radiative corrections to the Higgs boson mass [10–15]. Furthermore, it is intriguing that a weakly interacting, (meta)stable supersymmetric particle might make up some or all of the dark matter in the universe [16–18]. In addition, SUSY predicts that gauge couplings, as measured experimentally at the electroweak scale, unify at an energy scale $\mathcal{O}(10^{16})$GeV ("GUT scale") near the Planck scale [19–25].

In the minimal supersymmetric extension to the Standard Model, the so called MSSM [11,26,27], a supersymmetry transformation relates every fermion and gauge boson in the SM to a supersymmetric partner with half a unit of spin difference, but otherwise with the same properties and quantum numbers. These are the "sfermions": squarks ($\tilde{q}$) and sleptons ($\tilde{\ell}$, $\tilde{\nu}$), and the "gauginos". The MSSM Higgs sector contains two doublets, for up-type quarks and for down-type quarks and charged leptons respectively. After electroweak symmetry breaking, five Higgs bosons arise, of which two are charged. The supersymmetric partners of the Higgs doublets are known as "higgsinos." The charged weak gauginos and higgsinos mix to "charginos" ($\tilde{\chi}^{\pm}$), and the neutral ones mix to "neutralinos" ($\tilde{\chi}^{0}$). The SUSY partners of the gluons are known as "gluinos" ($\tilde{g}$). The fact that such particles are not yet observed leads to the conclusion that, if supersymmetry is realized, it is a broken symmetry. A description of SUSY in the form of an effective Lagrangian with only "soft" SUSY breaking terms and SUSY masses at the TeV scale maintains cancellation of quadratic divergences in particle physics models.

The phenomenology of SUSY is to a large extent determined by the SUSY breaking mechanism and the SUSY breaking scale. This determines the SUSY particle masses, the mass hierarchy, the field contents of physical particles, and their decay modes. In addition, phenomenology crucially depends on whether the multiplicative quantum number of R-parity [27], $R = (-1)^{3(B-L)+2S}$, where B and L are baryon and lepton numbers and S is the spin, is conserved or violated. If R-parity is conserved, SUSY particles (sparticles), which have odd R-parity, are produced in pairs and the decays of each SUSY particle must involve an odd number of lighter SUSY particles. The lightest SUSY particle (LSP) is then stable and often assumed to be a weakly interacting massive particle (WIMP). If R-parity is violated, new terms λ_{ijk}, λ'_{ijk} and λ''_{ijk} appear in the superpotential, where ijk are generation indices; λ-type couplings appear between lepton superfields only, λ''-type are between quark superfields only, and λ'-type couplings connect the two. R-parity violation implies lepton and/or baryon number violation. More details of the theoretical framework of SUSY are discussed elsewhere in this volume [28].

Today low-energy data from flavor physics experiments, high-precision electroweak observables as well as astrophysical data impose strong constraints on the allowed SUSY parameter space. Recent examples of such data include measurements of the rare B-meson decay $B_s \to \mu^+\mu^-$ [29] and accurate determinations of the cosmological dark matter relic density constraint [30,31].

These indirect constraints are often more sensitive to higher SUSY mass scales than experiments searching for direct sparticle production at colliders, but the interpretation of these results is often strongly model dependent. In contrast, direct searches for sparticle production at collider experiments are less subject to interpretation ambiguities and therefore they play a crucial role in the search for SUSY.

The discovery of a new scalar boson with a mass around 125 GeV compatible with a Higgs boson imposes constraints on SUSY, which are discussed elsewhere [28,32].

In this review we limit ourselves to direct searches, covering data analyses at LEP, HERA, the Tevatron and the LHC, with emphasis on the latter. For more details on LEP and Tevatron constraints, see earlier PDG reviews [33].

II.2. Experimental search program

The electron-positron collider LEP was operational at CERN between 1989 and 2000. In the initial phase, center-of-mass energies around the Z-peak were probed, but after 1995 the LEP experiments collected a significant amount of luminosity at higher center-of-mass energies, some 235 pb^{-1} per experiment at $\sqrt{s} \geq 204$ GeV, with a maximum $\sqrt{s}$ of 209 GeV.

Searches for new physics at e^+e^- colliders benefit from the clean experimental environment and the fact that momentum balance can be measured not only in the plane transverse to the beam, but also in the direction along the beam (up to the beam pipe holes), defined as the longitudinal direction. Searches at LEP are dominated by the data samples taken at the highest center-of-mass energies.

Significant constraints on SUSY have been set by the CDF and D0 experiments at the Tevatron, a proton-antiproton collider at a center-of-mass energy of up to 1.96 TeV. CDF and D0 have collected integrated luminosities between 10 and 11 fb^{-1} each up to the end of collider operations in 2011.

The electron-proton collider HERA provided collisions to the H1 and ZEUS experiments between 1992 and 2007, at a center-of-mass energy up to 318 GeV. A total integrated luminosity of approximately 0.5 fb^{-1} has been collected by each experiment. Since in ep collisions no annihilation process takes place, SUSY searches at HERA typically look for R-parity violating production of single SUSY particles.

The LHC has started proton-proton operation at a center-of-mass energy of 7 TeV in 2010. By the end of 2011 the experiments ATLAS and CMS had collected about 5 fb^{-1} of integrated luminosity each, and the LHCb experiment had collected approximately 1 fb^{-1}. In 2012, the LHC operated at a center-of-mass energy of 8 TeV, and ATLAS and CMS collected approximately 20 fb^{-1} each, whereas LHCb collected 2 fb^{-1}. In

2015, the LHC has started Run 2, with center-of-mass energy of 13 TeV.

Proton-(anti)proton colliders produce interactions at higher center-of-mass energies than those available at LEP, and cross sections of QCD-mediated processes are larger, which is reflected in the higher sensitivity for SUSY particles carrying color charge: squarks and gluinos. Large background contributions from Standard Model processes, however, pose challenges to trigger and analysis. Such backgrounds are dominated by multijet production processes, including, particularly at the LHC, those of top quark production, as well as jet production in association with vector bosons. The proton momentum is shared between its parton constituents, and in each collision only a fraction of the total center-of-mass energy is available in the hard parton-parton scattering. Since the parton momenta in the longitudinal direction are not known on an event-by-event basis, use of momentum conservation constraints in an analysis is restricted to the transverse plane, leading to the definition of transverse variables, such as the missing transverse momentum, and the transverse mass. Proton-proton collisions at the LHC differ from proton-antiproton collisions at the Tevatron in the sense that there are no valence anti-quarks in the proton, and that gluon-initiated processes play a more dominant role. The increased center-of-mass energy of the LHC compared to the Tevatron significantly extends the kinematic reach for SUSY searches. This is reflected foremost in the sensitivity for squarks and gluinos, but also for other SUSY particles.

The main production mechanisms of massive colored sparticles at hadron colliders are squark-squark, squark-gluino and gluino-gluino production; when "squark" is used "antisquark" is also implied. The typical SUSY search signature at hadron colliders contains high-p_{T} jets, which are produced in the decay chains of heavy squarks and gluinos, and significant missing momentum originating from the two LSPs produced at the end of the decay chain. Assuming R-parity conservation, the LSPs are neutral and weakly interacting massive particles which escape detection. Standard Model backgrounds with missing transverse momentum include leptonic W/Z-boson decays, heavy-flavor

decays to neutrinos, and multijet events that may be affected by instrumental effects such as jet mismeasurement.

Selection variables designed to separate the SUSY signal from the Standard Model backgrounds include H_{T}, $E_{\mathrm{T}}^{\mathrm{miss}}$, and m_{eff}. The quantities H_{T} and $E_{\mathrm{T}}^{\mathrm{miss}}$ refer to the measured transverse energy and missing transverse momentum in the event, respectively. They are usually defined as the scalar (H_{T}) and negative vector sum ($E_{\mathrm{T}}^{\mathrm{miss}}$) of the transverse jet energies or transverse calorimeter clusters energies measured in the event. The quantity m_{eff} is referred to as the effective mass of the event and is defined as $m_{\mathrm{eff}} = H_{\mathrm{T}} + |E_{\mathrm{T}}^{\mathrm{miss}}|$. The peak of the m_{eff} distribution for SUSY signal events correlates with the SUSY mass scale, in particular with the mass difference between the primary produced SUSY particle and the LSP [34], whereas the Standard Model backgrounds dominate at low m_{eff}. Additional reduction of multijet backgrounds can be achieved by demanding isolated leptons or photons in the final states; in such events the lepton or photon transverse momentum may be added to H_{T} or m_{eff} for further signal-background separation.

In the past few years alternative approaches have been developed to increase the sensitivity to pair production of heavy sparticles with masses around 1 TeV focusing on the kinematics of their decays, and to further suppress the background from multijet production. Prominent examples of these new approaches are searches using the α_{T} [35–39], *razor* [40], *stransverse mass* (m_{T2}) [41], and *contransverse mass* (m_{CT}) [42] variables.

II.3. Interpretation of results

Since the mechanism by which SUSY is broken is unknown, a general approach to SUSY via the most general soft SUSY breaking Lagrangian adds a significant number of new free parameters. For the minimal supersymmetric standard model, MSSM, *i.e.*, the model with the minimal particle content, these comprise 105 new parameters. A phenomenological analysis of SUSY searches leaving all these parameters free is not feasible. For the practical interpretation of SUSY searches at colliders several approaches are taken to reduce the number of free parameters.

One approach is to assume a SUSY breaking mechanism and lower the number of free parameters through the assumption of additional constraints. In particular in past years, interpretations of experimental results were predominately performed in constrained models of gravity mediated [43,44], gauge mediated [45,46], and anomaly mediated [47,48] SUSY breaking. Before the start of the LHC and even during its first year of operation, the most popular model for interpretation of collider based SUSY searches was the constrained MSSM (CMSSM) [43,49,50], which in the literature is also referred to as minimal supergravity, or MSUGRA. The CMSSM is described by five parameters: the common sfermion mass m_0, the common gaugino mass $m_{1/2}$, and the common trilinear coupling parameter A_0, all defined at the GUT scale, the ratio of the vacuum expectation values of the Higgs fields for up-type and down-type fermions $\tan\beta$, and the sign of the higgsino mass parameter μ, defined at the electroweak scale. In gauge mediation models, the paradigm of general gauge mediation (GGM) [51] is slowly replacing minimal gauge mediation, denoted traditionally as GMSB (gauge mediated SUSY breaking).

These constrained SUSY models are theoretically well motivated and provide a rich spectrum of experimental signatures. Therefore, they represent a useful framework to benchmark performance, compare limits or reaches and assess the expected sensitivity of different search strategies. However, with universality relations imposed on the soft SUSY breaking parameters, they do not cover all possible kinematic signatures and mass relations of SUSY. In such scenarios the squarks are often nearly degenerate in mass, in particular for the first and second generation. The exclusion of parameter space in the CMSSM and in CMSSM-inspired models is mainly driven by first and second generation squark production together with gluino production.

As shown in Fig. 1 [52] these processes possess the largest production cross sections in proton-proton collisions, and thus the LHC searches typically provide the tightest mass limits on these colored sparticles. This, however, implies that the allowed parameter space of constrained SUSY models today has been restrained significantly by searches from ATLAS and

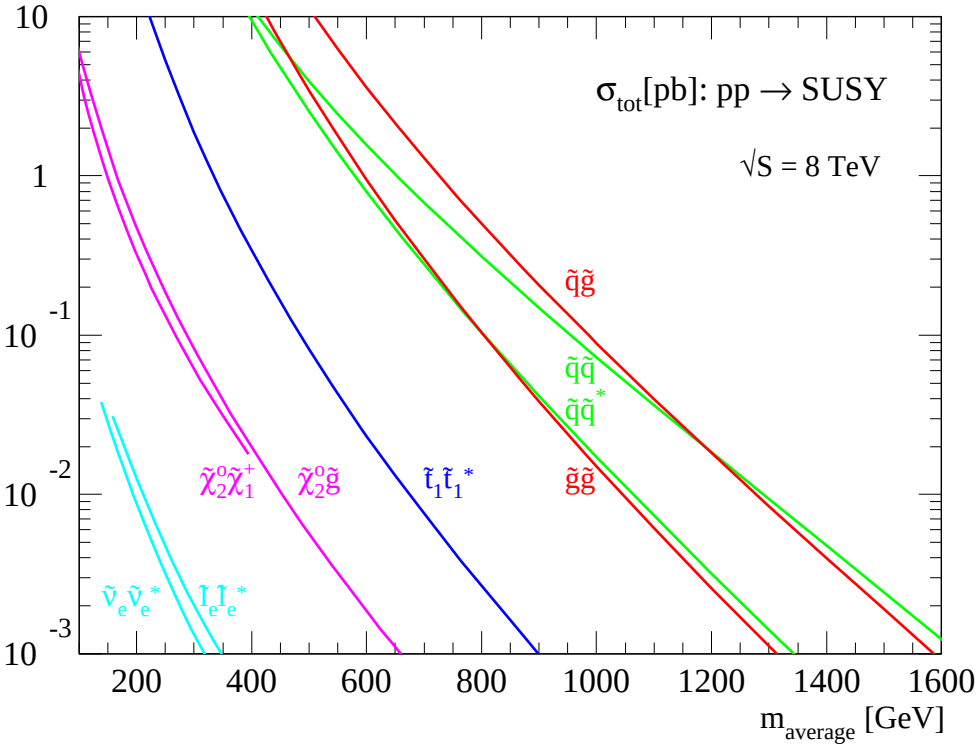

Figure 1: Cross sections for pair production of different sparticles as a function of their mass at the LHC for a center-of-mass energy of 8 TeV [52]. Typically the production cross section of colored squarks and gluinos is several orders of magnitude larger than the one for leptons or charginos. Except for the explicitly shown pair production of stops, production cross sections for squarks assumes mass degeneracy of left- and right-handed u, d, s, c and b squarks.

CMS. Furthermore, confronting the remaining allowed parameter space with other collider and non-collider measurements, which are directly or indirectly sensitive to contributions from SUSY, the overall compatibility of these models with all data is significantly worse than in the pre-LHC era (see section II.7 for further discussion), indicating that very constrained models like the CMSSM might no longer be good benchmark scenarios to solely characterize the results of SUSY searches at the LHC.

For these reasons, an effort has been made in the past years to complement the traditional constrained models with more flexible approaches.

One answer to study a broader and more comprehensive subset of the MSSM is via the phenomenological-MSSM, or pMSSM [53–55]. It is derived from the MSSM, using experimental data to eliminate parameters that are free in principle but have already been highly constrained by measurements of *e.g.*, flavor mixing and CP-violation. This effective approach reduces the number of free parameters in the MSSM to typically 19, making it a practical compromise between the full MSSM and highly constrained models such as the CMSSM.

Even less dependent on fundamental assumptions are interpretations in terms of so-called simplified models [56–59]. Such models assume a limited set of SUSY particle production and decay modes and leave open the possibility to vary masses and other parameters freely. Therefore, simplified models enable comprehensive studies of individual SUSY topologies, and are useful for optimization of the experimental searches over a wide parameter space. As a consequence, since 2011 ATLAS and CMS have adopted simplified models as the primary framework to provide interpretations of their searches. Today, almost every individual search provides interpretations of their results in one or even several simplified models that are characteristic of SUSY topologies probed by the analysis.

However, while these models are very convenient for the interpretation of individual SUSY production and decay topologies, care must be taken when applying these limits to more complex SUSY spectra. Therefore, in practise, simplified model limits are often used as an approximation of the constraints that can be placed on sparticle masses in more complex SUSY spectra. Yet, depending on the assumed SUSY spectrum, the sparticle of interest, and the considered simplified model limit, this approximation can lead to a significant mistake, typically an overestimation, in the assumed constraint on the sparticle mass (see for example [60]) . Only on a case-by-case basis can it be determined whether the limit of a given simplified model represents a good approximation of the true underlying constraint that can be applied on a sparticle mass in a complex SUSY spectrum. In the following, we will always point out

explicitly the assumptions that have entered the limits when quoting interpretations from simplified models.

This review covers results up to September 2015 and since none of the searches performed so far have shown significant excess above the SM background prediction, the interpretation of the presented results are exclusion limits on SUSY parameter space.

II.4. Exclusion limits on gluino and squark masses

Gluinos and squarks are the SUSY partners of gluons and quarks, and thus carry color charge. Limits on squark masses of the order 100 GeV have been set by the LEP experiments [61]. However, due to the colored production of these particles at hadron colliders (see e.g. Fig. 1), hadron collider experiments are able to set much tighter mass limits.

Pair production of these massive colored sparticles at hadron colliders generally involve both s-channel and t-channel parton-parton interactions. Since there is a negligible amount of bottom and top quark content in the proton, top- and bottom squark production proceeds through s-channel diagrams only with smaller cross sections. In the past, experimental analyses of squark and/or gluino production typically assumed the first and second generation squarks to be approximately degenerate in mass. However, in order to have even less model dependent interpretations of the searches, the experiments have started to also provide simplified model limits on individual first or second generation squarks.

Assuming R-parity conservation and assuming gluinos to be heavier than squarks, squarks will predominantly decay to a quark and a neutralino or chargino, if kinematically allowed. The decay may involve the lightest neutralino (typically the LSP) or chargino, but, depending on the masses of the gauginos, may involve heavier neutralinos or charginos. For pair production of first and second generation squarks, the simplest decay modes involve two jets and missing momentum, with potential extra jets stemming from initial state or final state radiation (ISR/FSR) or from decay modes with longer cascades. Similarly, gluino pair production leads to four jets and missing

momentum, and possibly additional jets from ISR/FSR or cascades. Associated production of a gluino and a (anti-)squark is also possible, in particular if squarks and gluinos have similar masses, typically leading to three or more jets in the final state. In cascades, isolated photons or leptons may appear from the decays of sparticles such as neutralinos or charginos. Final states are thus characterized by significant missing transverse momentum, and at least two, and possibly many more high p_{T} jets, which can be accompanied by one or more isolated objects like photons or leptons, including τ leptons, in the final state. Table 1 shows a schematic overview of characteristic final state signatures of gluino and squark production for different mass hierarchy hypotheses and assuming decays involving the lightest neutralino.

The main reference for ATLAS results in this section is the ATLAS Run 1 summary paper on squark and gluino production [62], while for CMS individual results are cited.

Table 1: Typical search signatures at hadron colliders for direct gluino and first- and second-generation squark production assuming different mass hierarchies.

Mass Hierarchy	Main Production	Dominant Decay	Typical Signature
$m_{\tilde{q}} \ll m_{\tilde{g}}$	$\tilde{q}\tilde{q}, \tilde{q}\bar{\tilde{q}}$	$\tilde{q} \to q\tilde{\chi}_1^0$	≥ 2 jets + $E_{\mathrm{T}}^{\mathrm{miss}}$ + X
$m_{\tilde{q}} \approx m_{\tilde{g}}$	$\tilde{q}\tilde{g}, \bar{\tilde{q}}\tilde{g}$	$\tilde{q} \to q\tilde{\chi}_1^0$	≥ 3 jets + $E_{\mathrm{T}}^{\mathrm{miss}}$ + X
		$\tilde{g} \to q\bar{q}\tilde{\chi}_1^0$	
$m_{\tilde{q}} \gg m_{\tilde{g}}$	$\tilde{g}\tilde{g}$	$\tilde{g} \to q\bar{q}\tilde{\chi}_1^0$	≥ 4 jets + $E_{\mathrm{T}}^{\mathrm{miss}}$ + X

II.4.1 Exclusion limits on the gluino mass

Limits set by the Tevatron experiments on the gluino mass assume the framework of the CMSSM, with $\tan\beta = 5$ (CDF) or $\tan\beta = 3$ (D0), $A_0 = 0$ and $\mu < 0$, and amount to lower limits of about 310 GeV for all squark masses, or 390 GeV for the case $m_{\tilde{q}} = m_{\tilde{g}}$ [63,64]. During the first year of physics operation of the LHC in 2010, these limits have been superseded by those provided by ATLAS and CMS.

Today, limits on the gluino mass have been set using up to approximately 20 fb^{-1} of data recorded at a center-of-mass energy of 8 TeV. As shown in Fig. 2, the ATLAS collaboration places limits for several searches in the framework of the CMSSM, assuming $\tan\beta = 30$, $A_0 = -2m_0$, and $\mu > 0$ [62]; these parameter values are chosen since they lead to a mass for the lightest Higgs boson compatible with 125 GeV in a large part of the $m_0 - m_{1/2}$ plane. For low m_0 the combination of the 0+1 lepton plus jets and missing momentum analyses provides the best sensitivity, while for values of m_0 above ≈ 1800 GeV a more dedicated search requiring zero or one isolated lepton accompanied with at least three jets identified to originate from bottom quarks (b-jets) takes over. The limits at low m_0 are mainly driven by squark-gluino and squark-squark production and at high m_0 gluino pair production dominates. As also indicated in Fig. 1, all other particle production modes do not play a significant role for limits in the CMSSM. In this constrained model gluino masses below around 1300 GeV are excluded by the ATLAS collaboration for all squark masses, while for equal squark and gluino masses, the limit is about 1700 GeV. Further details about the searches that are displayed in Fig. 2 can be obtained from the ATLAS summary paper on squark and gluino production [62].

Limits on the gluino mass have also been established in the framework of simplified models. Assuming only gluino pair production, in particular three primary decay chains of the gluino have been considered by the LHC experiments for interpretations of their search results. The first decay chain $\tilde{g} \to q\bar{q}\tilde{\chi}_1^0$ assumes gluino mediated production of first and second generation squarks which leads to four light flavor quarks in the final state. Therefore, inclusive all-hadronic analyses searching for multijet plus $E_{\text{T}}^{\text{miss}}$ final states are utilized to put limits on this simplified model. These limits are derived as a function of the gluino and neutralino (LSP) mass. As shown in Fig. 3 (upper left), using the cross section from next-to-leading order QCD corrections and the resummation of soft gluon emission at next-to-leading-logarithmic accuracy as reference, the CMS collaboration [65] excludes in this simplified model gluino masses

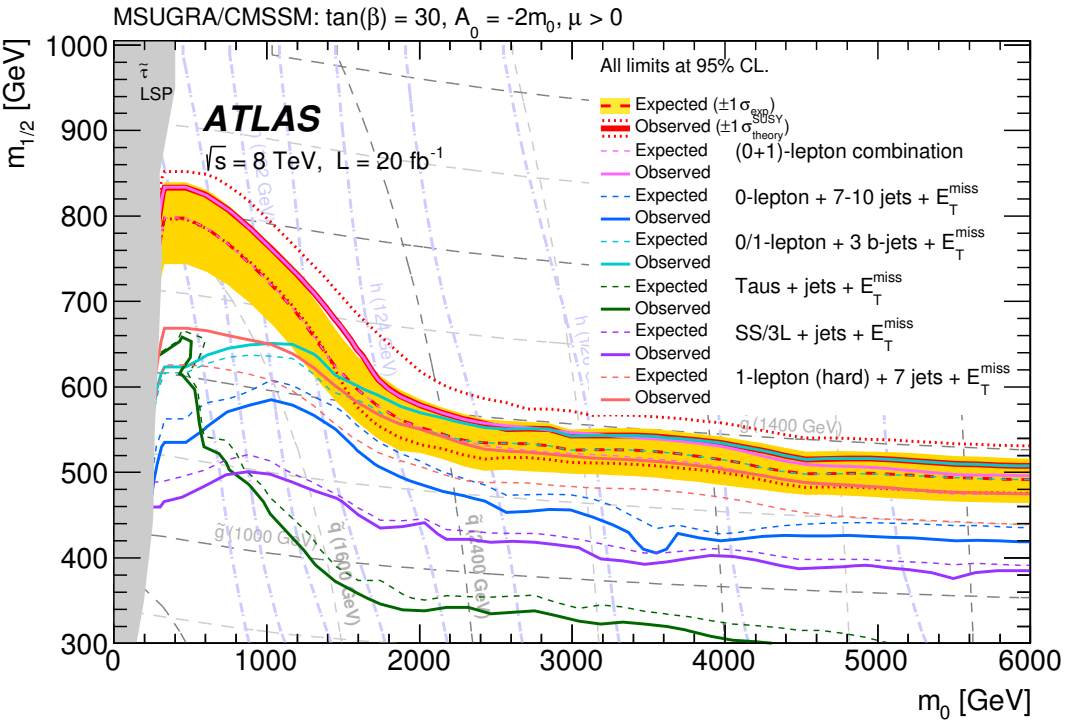

Figure 2: Limits, at 95% C.L., derived from several different ATLAS searches in the CMSSM parameters m_0 and $m_{1/2}$, assuming $\tan\beta = 30$, $A_0 = -2m_0$ and $\mu > 0$ [62].

below approximately 1300 GeV (see also [66–68]) , for a massless neutralino. In scenarios where neutralinos are not very light, the efficiency of the analyses is reduced by the fact that jets are less energetic, and there is less missing transverse momentum in the event. This leads to weaker limits when the mass difference $\Delta m = m_{\tilde{g}} - m_{\tilde{\chi}_1^0}$ is reduced. For example, for neutralino masses above about 550 GeV no limit on the gluino mass can be set for this decay chain. Therefore, limits on gluino masses are strongly affected by the assumption of the neutralino mass. Similar results for this simplified model have been obtained by ATLAS [62].

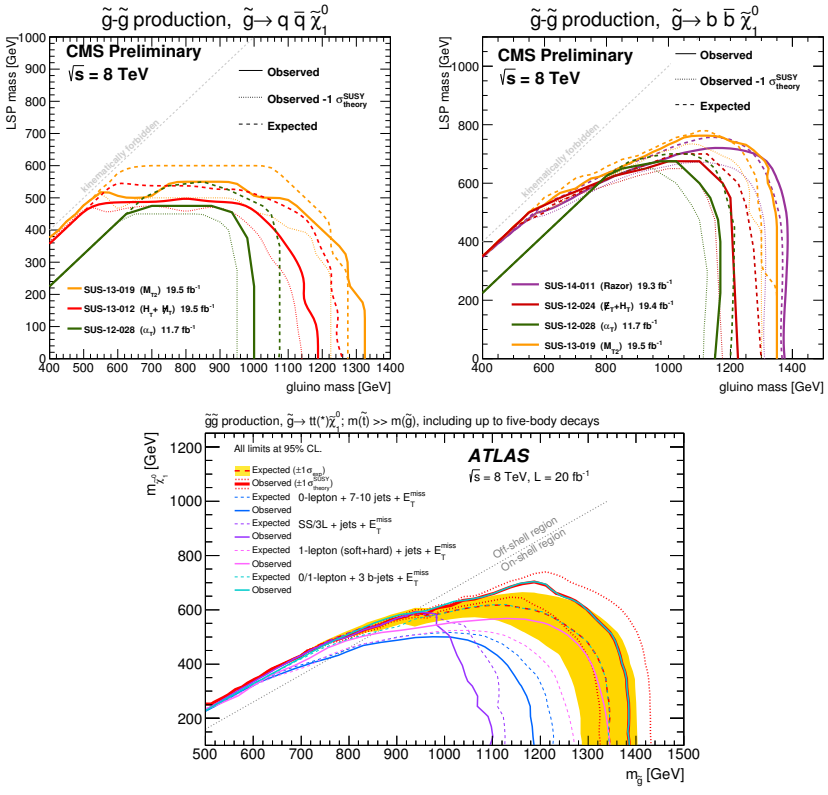

Figure 3: Upper mass limits, at 95% C.L., on gluino pair production for the decay chains $\tilde{g} \to q\bar{q}\tilde{\chi}_1^0$ (upper left) [65], $\tilde{g} \to b\bar{b}\tilde{\chi}_1^0$ (upper right) [66], and $\tilde{g} \to t\bar{t}\tilde{\chi}_1^0$ (lower middle) [62,157]. The limits are defined in the framework of simplified models assuming a single decay chain, (i.e. 100% branching fraction). The upper plots show limits from the CMS collaboration, while the displayed limits for $\tilde{g} \to t\bar{t}\tilde{\chi}_1^0$ are obtained from ATLAS searches. It should be note that the ATLAS results include both on-shell as well as off-shell production of gluino induced stop production (see text for details).

The second important decay chain of the gluino considered for interpretation in a simplified model is $\tilde{g} \to b\bar{b}\tilde{\chi}_1^0$. Here the decay is mediated via bottom squarks and thus leads to four jets from b quarks and $E_{\mathrm{T}}^{\mathrm{miss}}$ in the final state. Also for this topology inclusive all-hadronic searches provide the highest sensitivity. However, with four b quarks in the final state, the use of secondary vertex reconstruction for the identification of

jets originating from b quarks provides a powerful handle on the SM background. Therefore, in addition to a multijet plus $E_{\mathrm{T}}^{\mathrm{miss}}$ signature these searches also require several jets to be tagged as b-jets. As shown in Fig. 3 (upper right), for this simplified model CMS [66] excludes gluino masses below $\approx$ 1350 GeV for a massless neutralino, while for neutralino masses above $\approx$ 750 GeV no limit on the gluino mass can be set. Comparable limits for this simplified model are provided by searches from ATLAS [62].

Not only first and second generation squarks or bottom squarks may be the product of gluino decays but also, if kinematically allowed, top squarks via the decay $\tilde{g} \to \tilde{t}t$. This leads to a "four tops" final state $ttttt\tilde{\chi}_1^0\tilde{\chi}_1^0$ and defines the third important simplified model, $\tilde{g} \to t\bar{t}\tilde{\chi}_1^0$, characterizing gluino pair production. The topology of this decay is very rich in different experimental signatures: as many as four isolated leptons, four b-jets, several light flavor quark jets, and significant missing momentum from the neutrinos in the W decay and from the two neutralinos. Therefore, in contrast to the other two simplified models, dedicated searches optimized for this particular final state provide the best mass limit on the gluino for this simplified model. As shown in Fig. 3 (lower middle) [62,157], the ATLAS search requiring significant $E_{\mathrm{T}}^{\mathrm{miss}}$, zero or one isolated lepton, and at least three jets identified as b-jets [69] provides the strongest limit on the gluino mass in the on-shell region ($m_{\tilde{g}} > 2m_t + m_{\tilde{\chi}_1^0}$). At 95% C.L. it rules out a gluino mass below $\approx$ 1400 GeV for $m_{\tilde{\chi}_1^0} < 300$ GeV. For neutralino masses above $\approx$ 700 GeV, no limit can be placed on the gluino mass for this simplified model. A CMS search [70] also especially optimized for this decay topology by requiring one isolated lepton and high jet multiplicity obtains similar limits.

The ATLAS collaboration also provides limits for the off-shell region ($m_{\tilde{g}} < 2m_t + m_{\tilde{\chi}_1^0}$) of this decay. In the regions of parameter space where the mass difference between the gluino and the lightest neutralino is small, additional sensitivity is obtained from the same-sign search requiring 3 leptons in the final state. To place limits in this off-shell region only four-body ($\tilde{g} \to tWb\tilde{\chi}_1^0$ and five-body $\tilde{g} \to WbWb\tilde{\chi}_1^0$ are considered

as for higher multiplicities the gluinos do not decay promptly anymore and thus lead to a different signature topology. With this approach additional parameter space for gluino masses below about 950 GeV can excluded in the $m_{\tilde{g}} < 2m_t + m_{\tilde{\chi}_1^0}$ region.

When comparing the limits in Fig. 3 for the three different simplified models it becomes apparent that more parameter space can be excluded when the gluino decay chain is mediated via third generation squarks. The reason for this is the better control of the SM background by means of identification of b-jets as well as dedicated topology requirements like high jet multiplicity or isolated leptons for these special signatures. However, this variation in sensitivity of the searches for different gluino decay chains is also a clear indication that care must be taken when limits from these simplified models are applied to SUSY models possessing more complex underlying spectra.

If the gluino decay is suppressed, for example if squark masses are high, gluinos may live longer than typical hadronization times. It is expected that such gluinos will hadronize to semi-stable strongly interacting particles known as R-hadrons. Searches for R-hadrons exploit the typical signature of stable charged massive particles in the detector. As shown in Fig. 4, the CMS experiment excludes semi-stable gluino R-hadrons with masses below approximately 1.3 TeV [71]. The limits depend on the probability for gluinos to form bound states known as gluinoballs, as these are neutral and not observed in the tracking detectors. Similar limits are obtained by the ATLAS experiment [72]. Limits of about 1 TeV are set in the scenario of R-hadron decays inside the detector, for $c\tau$ ranging from 1 to 1000 mm [73].

Alternatively, since such R-hadrons are strongly interacting, they may be stopped in the calorimeter or in other material, and decay later into energetic jets. These decays are searched for by identifying the jets outside the time window associated with bunch-bunch collisions [74–76]. The latest ATLAS analysis [75] based on the full 2011 and 2012 data set combined (28 fb^{-1}) places limits at 95% C.L. on gluino production over almost 16 orders of magnitude in gluino lifetime. For $m_{\tilde{\chi}_1^0} > 100$ GeV,

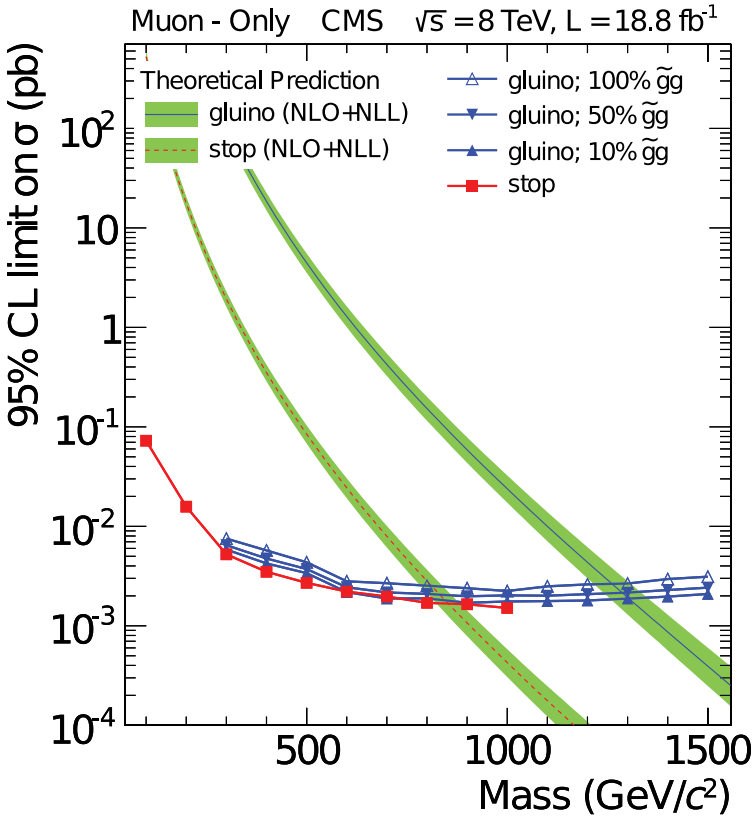

Figure 4: Observed 95% C.L. upper limits on the cross section for (semi-)stable top squarks or gluinos [71]. For gluinos, different fractions of gluinoball states produced after hadronization scenarios are indicated. The observed limits are compared with the predicted theoretical cross sections where the bands represent the theoretical uncertainties on the cross section values.

assuming a 100% branching fraction for gluino decay to gluon (or $q\bar{q}$) + neutralino, gluinos with lifetimes from 10 μs to 1000 s and $m_{\tilde{g}} < 832$ GeV are excluded. When SUSY spectra are compressed, this limit weakens to an exclusion of $m_{\tilde{g}} < 545$ GeV for $m_{\tilde{g}} - m_{\tilde{\chi}^0_1} < 100$ GeV.

In summary, for interpretations in the CMSSM, simplified models, and semi-stable R-hadrons, the best limits on the gluino mass range from around 1200 GeV to about 1400 GeV, while for interpretations in the context of stopped R-hadrons the limit on $m_{\tilde{g}}$ is around 850 GeV. All these limits weaken significantly for

compressed SUSY spectra when the mass difference $m_{\tilde{g}} - m_{\tilde{\chi}_1^0}$ is reduced.

R-parity violating gluino decays are searched for in a number of final states. Searches in multilepton final states set lower mass limits of 1 to 1.4 TeV, depending on neutralino mass and lepton flavor, on decays mediated by λ and λ' couplings [77,78], assuming prompt decays. Searches for displaced vertices are sensitive to non-prompt decays [73]. Multijet final states have been used to search for fully hadronic gluino decays involving λ'', by CDF [79], ATLAS [80] and CMS [81]. Lower mass limits range between 800 and 1000 GeV depending on neutralino mass and flavor content of the final state.

II.4.2. Exclusion limits on first and second generation squark masses

Limits on first and second generation squark masses set by the Tevatron experiments assume the CMSSM model, and amount to lower limits of about 380 GeV for all gluino masses, or 390 GeV for the case $m_{\tilde{q}} = m_{\tilde{g}}$ [63,64].

At the LHC, limits on squark masses have been set using up to approximately 20 fb^{-1} of data at 8 TeV. As shown in Fig. 2, the ATLAS collaboration [62] excludes in the framework of the CMSSM squark masses below ≈ 1600 GeV for all gluino masses. For equal squark and gluino masses, the limit is about 1700 GeV.

Interpretations in simplified models are typically characterizing squark pair production with only one decay chain of $\tilde{q} \to q\tilde{\chi}_1^0$. Here it is assumed that the left and right-handed $\tilde{u}$, $\tilde{d}$, $\tilde{s}$ and $\tilde{c}$ squarks are degenerate in mass. Furthermore, it is assumed that the mass of the gluino is very high and thus contributions of the corresponding t-channel diagrams to squark pair production are negligible. Therefore, the total production cross section for this simplified model is eight times the production cross section of an individual squark (e.g. $\tilde{u}_L$). The CMS collaboration provides interpretations using different all-hadronic searches for this simplified model. As displayed in Fig. 5, best observed exclusion is obtained from the analysis using the m_{T2} variable [65], which excludes squark masses just below 925 GeV for a light neutralino. The effects of heavy

neutralinos on squark limits are similar to those discussed in the gluino case (see section II.4.1) and only for neutralino masses below ≈ 350 GeV squark masses can be excluded. Results from the ATLAS collaboration [62] for this simplified model are similar.

For the same analysis ATLAS also provides an interpretation of their search result in a simplified model assuming strong production of first and second generation squarks in association with gluinos. This interpretation excludes squark masses below ≈ 1400 GeV for all gluino masses as well as gluino masses below ≈ 1400 GeV for all squark masses. For equal squark and gluino masses, the limit is about 1700 GeV and therefore very similar to limits provided in the CMSSM.

If the assumption of mass degenerate first and second generation squarks is dropped and only the production of a single light squark is assumed, the limits weaken significantly. This is shown as the much smaller exclusion region in Fig. 5, which represents the 95% C.L. upper limit of pair production of a single light squark, with the gluino and all other squarks decoupled to very high masses. With a best observed squark mass limit of only ≈ 575 GeV for a massless neutralino and a neutralino mass of ≈ 120 GeV above which no squark mass limit can be placed, the exclusion reach of the LHC experiments for single light squark is rather weak. It should be noted that this limit is not a result of a simple scaling of the above mentioned mass limits assuming eightfold mass degeneracy but it also takes into account that for an eight times lower production cross section the analyses must probe kinematic regions of phase space that are closer to the ones of SM background production. Since signal acceptance and the ratio of expected signal to SM background events of the analyses are typically worse in this region of phase space not only the 1/8 reduction in production cross section but also a worse analysis sensitivity are responsible for the much weaker limit on single squark pair production.

For single light squarks ATLAS also reports results of a dedicated search for pair production of scalar partners of charm quarks [82]. Assuming that the scalar-charm state exclusively

decays into a charm quark and a neutralino, scalar-charm masses up to 490 GeV are excluded for neutralino masses below 200 GeV.

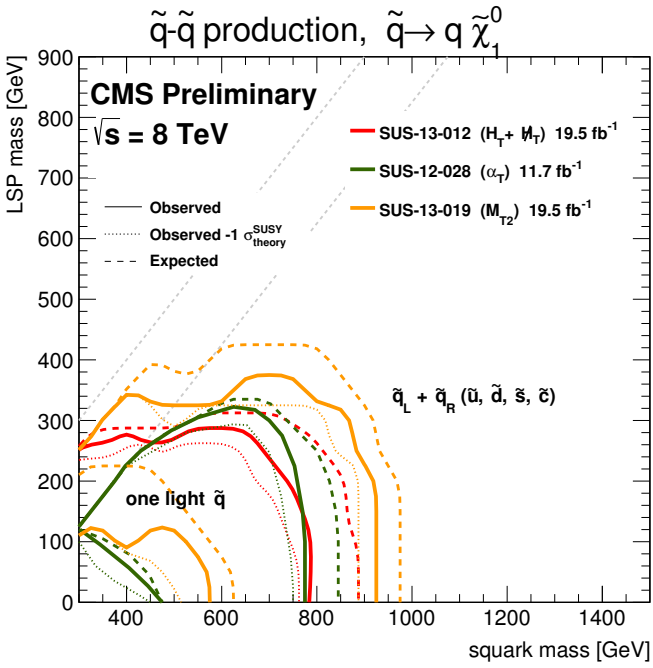

Figure 5: 95% C.L. exclusion contours in the squark-neutralino mass plane defined in the framework of simplified models assuming a single decay chain of $\tilde{q} \to q\tilde{\chi}_1^0$ [65]. Two assumptions for the squark pair production cross sections are displayed; a) eightfold degeneracy for the masses of the first and second generation squarks and b) only one light flavor squark.

R-parity violating production of single squarks via a λ'-type coupling has been studied at HERA. In such models, a lower limit on the squark mass of the order of 275 GeV has been set for electromagnetic-strength-like couplings $\lambda' = 0.3$ [83]. At the LHC, both prompt [77,78] and non-prompt [73,84] R-parity violating squark decays have been searched for, but no signal was found. Squark mass limits are very model-dependent.

II.4.3. Exclusion limits on third generation squark masses

SUSY at the TeV-scale is often motivated by naturalness arguments, most notably as a solution to stabilize quadratic divergences in radiative corrections to the Higgs boson mass. In this context, the most relevant terms for SUSY phenomenology arise from the interplay between the masses of the third generation squarks and the Yukawa coupling of the top quark to the Higgs boson. This motivates a potential constraint on the masses of the top squarks and the left-handed bottom squark. Due to the large top quark mass, significant mixing between $\tilde{t}_{\mathrm{L}}$ and $\tilde{t}_{\mathrm{R}}$ is expected, leading to a lighter mass state $\tilde{t}_1$ and a heavier mass state $\tilde{t}_2$. In the MSSM, the lightest top squark ($\tilde{t}_1$) can be the lightest squark.

The discovery of a Higgs boson at a mass around 125 GeV has consequences for third generation squarks in the MSSM, which are discussed elsewhere [28]. As a result, and in the absence of a SUSY discovery so far, searches for third generation squark production have become a major focus of the SUSY search program at the LHC. For this reason direct and gluino mediated top and/or bottom squark production processes, leading to experimental signatures that are rich in jets originating from bottom quarks, are either subject of re-interpretation of inclusive analyses or targets for dedicated searches. The latter ones have become especially important for searches of direct top squark production.

Direct production of top and bottom squark pairs at hadron colliders is suppressed with respect to first generation squarks, due to the absence of t and b quarks in the proton (see e.g. the example of direct top squark production in Fig. 1). At the LHC, assuming eightfold mass degeneracy for light flavor squarks as reference, this suppression is at the level of two orders of magnitude for top and bottom squark masses of around 600 GeV. Moreover, at the LHC, there is a very large background of top quark pair production, making especially the experimental analysis of top squark pair production a challenge.

The main reference for ATLAS results in this section is the summary paper for Run1 searches for direct pair production

of third-generation squarks [85], while for CMS individual references are cited.

Bottom squarks are expected to decay predominantly to $b\tilde{\chi}^0$ giving rise to the characteristic multi b-jet and $E_{\mathrm{T}}^{\mathrm{miss}}$ signature. Direct production of bottom squark pairs has been studied at the Tevatron and at the LHC. Limits from the Tevatron are $m_{\tilde{b}} > 247$ GeV for a massless neutralino [86,87]. Using the 2011 data the LHC experiments were able to surpass these limits and based on the full 2012 data set, as shown in Fig. 6, using an all-hadronic search requiring significant $E_{\mathrm{T}}^{\mathrm{miss}}$ and two jets reconstructed as b-jets in combination with a dedicated mono-jet analysis, ATLAS has set a limit of $m_{\tilde{b}} >\approx 650$ GeV for the same scenario. For $m_{\tilde{\chi}_1^0} \approx 280$ GeV or higher no limit can be placed on direct bottom squark pair production in this simplified model [85]. The addition of the mono-jet topology increases the sensitivity for compressed spectra allowing for an exclusion of up to $m_{\tilde{b}} \approx 280$ GeV along the diagonal. The latest CMS results for this simplified model are featured in [65–68,88] and exhibit a similar reach.

Further bottom squark decay modes have also been studied by ATLAS and CMS. For example, in a simplified model for the $\tilde{b} \to t\tilde{\chi}^{\pm}$ decay mode, bottom squark quark masses below approximately 450 GeV are excluded [85,88,89].

The top squark decay modes depend on the SUSY mass spectrum, and on the $\tilde{t}_{\mathrm{L}}$-$\tilde{t}_{\mathrm{R}}$ mixture of the top squark mass eigenstate. If kinematically allowed, the two-body decays $\tilde{t} \to t\tilde{\chi}^0$ (which requires $m_{\tilde{t}} - m_{\tilde{\chi}^0} > m_t$) and $\tilde{t} \to b\tilde{\chi}^{\pm}$ (which requires $m_{\tilde{t}} - m_{\tilde{\chi}^{\pm}} > m_b$) are expected to dominate. If not, the top squark decay may proceed either via the two-body decay $\tilde{t} \to c\tilde{\chi}^0$ or through $\tilde{t} \to bf\bar{f}'\tilde{\chi}^0$ (where f and $\bar{f}'$ denote a fermion-antifermion pair with appropriate quantum numbers). For $m_{\tilde{t}} - m_{\tilde{\chi}^0} > m_b$ the latter decay chain represents a four-body decay with a W boson, charged Higgs H, slepton $\tilde{\ell}$, or light flavor squark $\tilde{q}$, exchange. If the exchanged W boson and/or sleptons are kinematically allowed to be on-shell ($m_{\tilde{t}} - m_{\tilde{\chi}^{\pm}} > m_b + m_W$ and/or $m_{\tilde{t}} - m_{\tilde{\ell}} > m_b$), the three-body decays $\tilde{t} \to Wb\tilde{\chi}^0$ and/or $\tilde{t} \to bl\tilde{\ell}$ will become dominant.

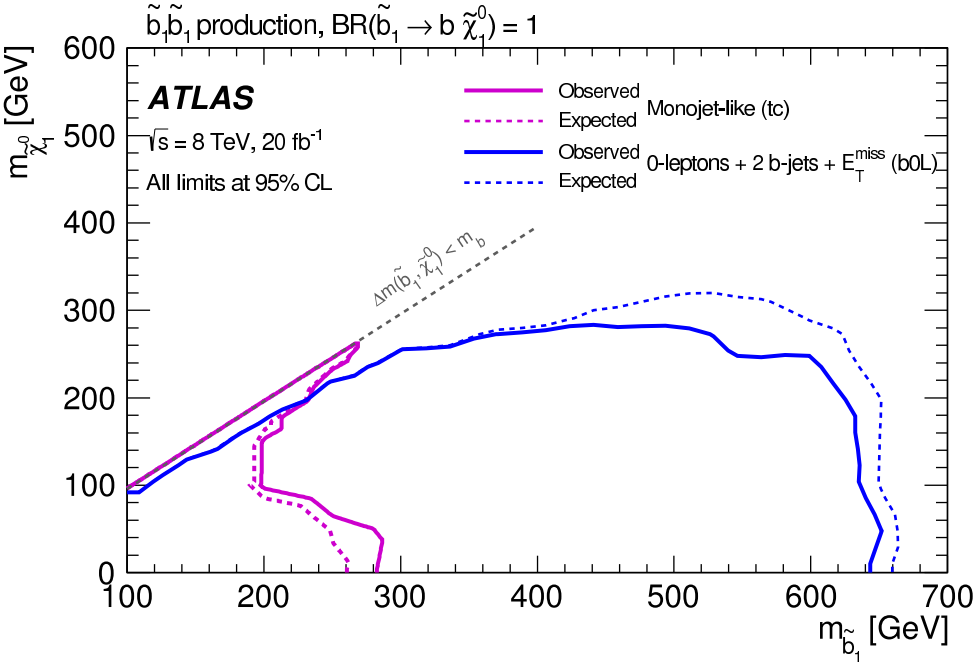

Figure 6: 95% C.L. exclusion contours in the sbottom-neutralino mass plane defined in the framework of a simplified model assuming a single decay chain of $\tilde{b} \to b\tilde{\chi}_1^0$ [85].

For further discussion on top squark decays see for example Ref. [90].

Limits from LEP on the $\tilde{t}_1$ mass are $m_{\tilde{t}} > 96$ GeV in the charm plus neutralino final state, and > 93 GeV in the lepton, b-quark and sneutrino final state [61].

The Tevatron experiments have performed a number of searches for top squarks, often assuming direct pair production. In the $b\ell\tilde{\nu}$ decay channel, and assuming a 100% branching fraction, limits are set as $m_{\tilde{t}} > 210$ GeV for $m_{\tilde{\nu}} < 110$ GeV and $m_{\tilde{t}} - m_{\tilde{\nu}} > 30$ GeV, or $m_{\tilde{t}} > 235$ GeV for $m_{\tilde{\nu}} < 50$ GeV [91,92]. In the $\tilde{t} \to c\tilde{\chi}^0$ decay mode, a top squark with a mass below 180 GeV is excluded for a neutralino lighter than 95 GeV [93,94]. In both analyses, no limits on the top squark can be set for heavy sneutrinos or neutralinos. In the $\tilde{t} \to b\tilde{\chi}_1^{\pm}$ decay channel, searches for a relatively light top squark have been performed in the dilepton final state [95,96]. The CDF experiment sets limits in the $\tilde{t} - \tilde{\chi}_1^0$ mass plane for various branching fractions

of the chargino decay to leptons and for two value of $m_{\tilde{\chi}_1^\pm}$. For $m_{\tilde{\chi}_1^\pm} = 105.8$ GeV and $m_{\tilde{\chi}_1^0} = 47.6$ GeV, top squarks between 128 and 135 GeV are excluded for W-like leptonic branching fractions of the chargino.

The LHC experiments have improved these limits substantially. As shown in the left plot of Fig. 7, limits on the top squark mass assuming a simplified model with a single decay chain of $\tilde{t} \to t\tilde{\chi}_1^0$ reach up to about 700 GeV for light neutralinos, while for $m_{\tilde{\chi}_1^0}$ >270 GeV no limits can be provided. The most important searches for this top squark decay topology are dedicated searches requiring zero or one isolated lepton, modest $E_{\mathrm{T}}^{\mathrm{miss}}$, and four or more jets out of which at least one jet must be reconstructed as b-jet [97,98]. To increase the sensitivity to this decay topology different signal regions are considered in these ATLAS analyses. Searches from the CMS collaboration requiring one isolated lepton and using a boosted decision tree for a dedicated optimization in the $m_{\tilde{t}} - m_{\tilde{\chi}_1^0}$ plane [99] or all-hadronic searches [65–68,88] provide comparable limits for this simplified model.

Assuming that the top squark decay exclusively proceeds via the chargino mediated decay chain $\tilde{t} \to b\tilde{\chi}_1^\pm$, $\tilde{\chi}_1^\pm \to W^{\pm(*)}\tilde{\chi}_1^0$ yields stop mass exclusion limits that vary strongly with the assumptions made on the $\tilde{t} - \tilde{\chi}_1^\pm - \tilde{\chi}_1^0$ mass hierarchy. As shown in the right plot of Fig. 7, above the universal chargino mass limit of $m_{\tilde{\chi}_1^\pm} > 103.5$ GeV from LEP (see section II.5.1) the strongest limits are placed for nearly mass degenerate chargino and neutralinos. For $m_{\tilde{\chi}_1^\pm} - m_{\tilde{\chi}_1^0}$ >5 GeV, a stop mass of $\approx$ 650 GeV for a light $\tilde{\chi}_1^0$ is excluded, while no limit can be placed for $m_{\tilde{\chi}_1^0} > 280$ GeV [85]. These limits, however, can weaken significantly when other assumptions about the mass hierarchy are imposed. For example, if the chargino becomes nearly mass degenerate with the top squark the key experimental signature turns from an all-hadronic final state with b-jets and $E_{\mathrm{T}}^{\mathrm{miss}}$ into a multi-lepton and $E_{\mathrm{T}}^{\mathrm{miss}}$ topology yielding significantly weaker limits for this top squark decay. As for the decay with top quarks in the final state, CMS [88,99] also provides comparable limits for this decay chain.

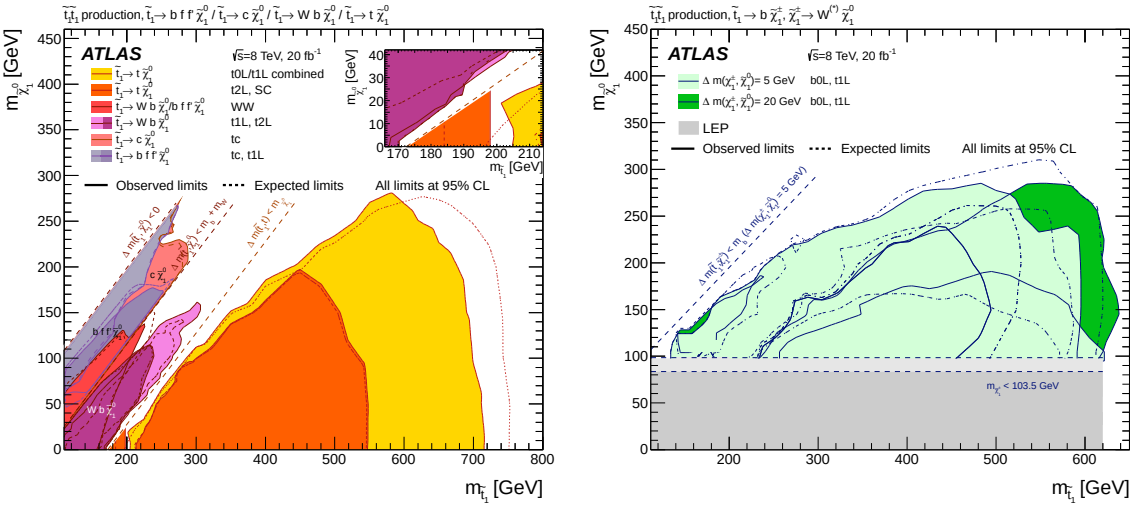

Figure 7: 95% C.L. exclusion contours in the $m_{\tilde{t}} - m_{\tilde{\chi}_1^0}$ plane for different top squark decay chains and different searches from the ATLAS collaboration [85]. The left plot shows simplified model limits for three different decay chains; $\tilde{t} \to c\tilde{\chi}_1^0$ (W and t forbidden), $\tilde{t} \to Wb\tilde{\chi}_1^0$ (t forbidden), and $\tilde{t} \to t\tilde{\chi}_1^0$ (t allowed), which represent three different kinematic regions of the top squark decay. The right plot shows simplified model limits for the top decay chain via a chargino: $\tilde{t} \to b\tilde{\chi}_1^{\pm}$, $\tilde{\chi}_1^{\pm} \to W^{\pm(*)}\tilde{\chi}_1^0$ for different $m_{\tilde{\chi}_1^{\pm}} - m_{\tilde{\chi}_1^0}$.

If the decays $\tilde{t} \to t\tilde{\chi}_1^0$ and $\tilde{t} \to b\tilde{\chi}_1^{\pm}$, $\tilde{\chi}_1^{\pm} \to W^{\pm(*)}\tilde{\chi}_1^0$ are kinematically forbidden, the decay chains $\tilde{t} \to Wb\tilde{\chi}^0$ and $\tilde{t} \to c\tilde{\chi}^0$ can become important. As shown in the left plot of Fig. 7,the one-lepton ATLAS search provides for the kinematic region $m_{\tilde{t}} - m_{\tilde{\chi}^{\pm}} > m_b + m_W$ upper limits on top squark mass of ≈ 300 GeV for a neutralino lighter than ≈ 170 GeV [85], while the boosted decision tree based CMS analysis pushes this limit to about 320 GeV for neutralino masses below ≈ 200 GeV [99]. For the kinematic region in which even the production of real W bosons is not allowed, ATLAS and CMS improves the Tevatron limit on $\tilde{t} \to c\tilde{\chi}^0$ substantially. Based on a combination of a monojet analysis and a dedicated charm quark identification algorithm, away from the kinematic boundary a top squark with a mass below 260 GeV is excluded by the ATLAS analysis

for a neutralino lighter than 230 GeV [85]. Along the kinematic boundary for the $\tilde{t} \to c\tilde{\chi}^0$ decay the ATLAS monojet results even excludes top squark masses below $m_{\tilde{\chi}_1^0} \approx 260$ GeV. The corresponding CMS results [88] exhibit similar exclusions. The other decay chain relevant in this phase region is $\tilde{t} \to bf\bar{f}'\tilde{\chi}^0$. Here the ATLAS one-lepton search [85] excludes up to $m_{\tilde{t}} \approx 250$ GeV for $m_{\tilde{\chi}_1^0}$ below 180 GeV, while the mono-jet excludes at the kinematic boundary top squarks below $m_{\tilde{\chi}^\pm}$ below 260 GeV. Also for this decay chain CMS [88] provides similar results.

In general, the variety of top squark decay chains in the phase space region where $\tilde{t} \to t\tilde{\chi}_1^0$ is kinematically forbidden represents a challenge for the experimental search program. As, for example, shown in the inlay of the left plot of Fig. 7 there are still regions in phase space for which the searches do not yet possess enough sensitivity to probe them. Additional data and more refined analyses will be required to also close these gaps.

R-parity violating production of single top squarks has been searched for at LEP, HERA, and the Tevatron. For example, an analysis from the ZEUS collaboration [100] makes an interpretation of its search result assuming top squarks to be produced via a λ' coupling and decay either to $b\tilde{\chi}_1^\pm$ or R-parity-violating to a lepton and a jet. Limits are set on λ'_{131} as a function of the top squark mass in an MSSM framework with gaugino mass unification at the GUT scale. The search for top squark pair production in the context of R-parity violating supersymmetry has now also become a focus point for searches at the LHC. Recently the CMS collaboration has performed a search for top squarks using a variety of multilepton final states [101]. It provides lower limits on the top squark mass in models with non-zero leptonic R-parity violating couplings λ_{122} and λ_{233}. For a bino mass of 200 GeV, these limits are 1020 GeV and 820 GeV, respectively. The analysis also provides limits in a model with the semileptonic R-parity violating coupling λ'_{233}. The λ'-mediated top squark decay $\tilde{t} \to b\ell$ has been studied by ATLAS for prompt decays [102], and by CMS for non-prompt decays [103]. The fully hadronic R-parity violating top squark decay $\tilde{t} \to bs$, involving λ'', has been searched for by ATLAS [104], and a lower top squark mass limit of 310 GeV

was set in this decay mode. CMS [105] have searched for a top squark decay to a bottom quark and a light-flavor quark, and excludes top squarks with masses between 200 and 385 GeV in this decay mode.

Top squarks can also be long-lived and hadronize to a R-hadron, for example in the scenario where the top squark is the next-to-lightest SUSY particle (NLSP), with a small mass difference to the LSP. Searches for massive stable charged particles are sensitive to such top squarks. As shown in Fig. 4, the CMS analysis [71] sets limits $m_{\tilde{t}} > 800$ GeV in such scenarios, while ATLAS [72] reports limits of $m_{\tilde{t}} > 900$ GeV. Limits from the Tevatron are about $m_{\tilde{t}} > 300$ GeV [106,107].

It should be noted that limits discussed in this section belong to different top and bottom squark decay channels, different sparticle mass hierarchies, and different simplified decay scenarios. Therefore, care must be taken when interpreting these limits in the context of more complete SUSY models.

II.4.4. Summary of exclusion limits on squarks and gluinos assuming R-Parity conservation

A summary of the most important squark and gluino mass limits for different interpretation approaches assuming R-parity conservation is shown in Table 2.

For gluino masses rather similar limits, ranging from 1.2 TeV to 1.4 TeV, are obtained from different model assumptions indicating that the LHC is indeed probing for a large region in SUSY parameter space direct gluino production at the 1 TeV scale and beyond. However, for neutralino masses above approximately 700 GeV in the best case, ATLAS and CMS searches cannot place any limits on the gluino mass.

Limits on direct squark production, on the other hand, depend strongly on the chosen model. Especially for direct production of top squarks there are still large regions in parameter space where masses below 0.5 TeV cannot be excluded. This is also true for first and second generation squarks when only one single squark is considered. Furthermore, for neutralino masses above $\approx$ 300 GeV no limit on any direct squark production scenario can be placed by the LHC.

e 2: Summary of squark mass and gluino mass limits using different interpre
oaches assuming R-parity conservation. Masses in this table are provided in GeV. F
ls about assumption and analyses from which these limits are obtained are discussed
sponding sections of the text.

Model	Assumption	$m_{\tilde{q}}$	$m_{\tilde{g}}$
CMSSM	$m_{\tilde{q}} \approx m_{\tilde{g}}$	≈ 1700	≈ 1700
	all $m_{\tilde{q}}$	-	≈ 1300
	all $m_{\tilde{g}}$	≈ 1600	-
Simplified model $\tilde{g}\tilde{q}, \tilde{g}\bar{\tilde{q}}$	$m_{\tilde{\chi}_1^0}= 0$, $m_{\tilde{q}} \approx m_{\tilde{g}}$	≈ 1700	≈ 1700
	$m_{\tilde{\chi}_1^0}= 0$, all $m_{\tilde{q}}$	-	≈ 1400
	$m_{\tilde{\chi}_1^0}= 0$, all $m_{\tilde{g}}$	≈ 1400	-
Simplified models $\tilde{g}\tilde{g}$			
$\tilde{g} \to q\bar{q}\tilde{\chi}_1^0$	$m_{\tilde{\chi}_1^0} =0$	-	≈ 1300
	$m_{\tilde{\chi}_1^0} >\approx 550$	-	no limit
$\tilde{g} \to b\bar{b}\tilde{\chi}_1^0$	$m_{\tilde{\chi}_1^0} =0$	-	≈ 1350
	$m_{\tilde{\chi}_1^0} >\approx 750$	-	no limit
$\tilde{g} \to t\bar{t}\tilde{\chi}_1^0$	$m_{\tilde{\chi}_1^0} =0$	-	≈ 1400
	$m_{\tilde{\chi}_1^0} >\approx 700$	-	no limit
Simplified models $\tilde{q}\tilde{q}$			
$\tilde{q} \to q\tilde{\chi}_1^0$	$m_{\tilde{\chi}_1^0} =0$	≈ 925	-
	$m_{\tilde{\chi}_1^0} >\approx 350$	no limit	-
$\tilde{u}_L \to q\tilde{\chi}_1^0$	$m_{\tilde{\chi}_1^0} =0$	≈ 575	-
	$m_{\tilde{\chi}_1^0} >\approx 120$	no limit	-
$\tilde{b} \to b\tilde{\chi}_1^0$	$m_{\tilde{\chi}_1^0} =0$	≈ 650	-
	$m_{\tilde{\chi}_1^0} >\approx 280$	no limit	-
$\tilde{t} \to t\tilde{\chi}_1^0$	$m_{\tilde{\chi}_1^0} =0$	≈ 700	-
	$m_{\tilde{\chi}_1^0} >\approx 270$	no limit	-
$\tilde{t} \to b\tilde{\chi}_1^\pm$	$m_{\tilde{\chi}_1^0} =0$	≈ 650	-
	$m_{\tilde{\chi}_1^0} >\approx 280$	no limit	-
$\tilde{t} \to Wb\tilde{\chi}_1^0$	$m_{\tilde{\chi}_1^0} <\approx 200$	≈ 320	-
$\tilde{t} \to c\tilde{\chi}_1^0$	$m_{\tilde{\chi}_1^0} <\approx 230$	≈ 260	-
	$m_{\tilde{t}} \approx m_{\tilde{\chi}_1^0}$	≈ 260	-
$\tilde{t} \to bff'\tilde{\chi}_1^0$	$m_{\tilde{\chi}_1^0} <\approx 180$	≈ 250	-
	$m_{\tilde{t}} \approx m_{\tilde{\chi}_1^0}$	≈ 260	-

II.5. Exclusion limits on the masses of charginos and neutralinos

Charginos and neutralinos result from mixing of the charged wino and higgsino states, and the neutral bino, wino and higgsino states, respectively. The mixing is determined by a limited number of parameters. For charginos these are the wino mass parameter M_2, the higgsino mass parameter μ, and $\tan\beta$, and for neutralinos these are the same parameters plus the bino mass parameter M_1. The mass states are four charginos $\tilde{\chi}_1^+$, $\tilde{\chi}_1^-$, $\tilde{\chi}_2^+$ and $\tilde{\chi}_2^-$, and four neutralinos $\tilde{\chi}_1^0$, $\tilde{\chi}_2^0$, $\tilde{\chi}_3^0$ and $\tilde{\chi}_4^0$, ordered in increasing mass. The mass states are superpositions of the bino, wino and higgsino states. If any of the parameters M_1, M_2 or μ happened to be substantially smaller than the others, the chargino and neutralino composition would be dominated by specific states, which are referred to as bino-like ($M_1 \ll M_2, \mu$), wino-like ($M_2 \ll M_1, \mu$), or higgsino-like ($\mu \ll M_1, M_2$). If gaugino mass unification at the GUT scale is assumed, a relation between M_1 and M_2 at the electroweak scale follows: $M_1 = 5/3 \tan^2\theta_W M_2 \approx 0.5 M_2$, with θ_W the weak mixing angle. Charginos and neutralinos carry no color charge, and only have electroweak couplings (neglecting gravity).

II.5.1. Exclusion limits on chargino masses

If kinematically allowed, two body decay modes such as $\tilde{\chi}^\pm \to \tilde{f}\bar{f}'$ (including $\ell\tilde{\nu}$ and $\tilde{\ell}\nu$) are dominant. If not, three body decay $\tilde{\chi}^\pm \to f\bar{f}'\tilde{\chi}^0$ are mediated through virtual W bosons or sfermions. If sfermions are heavy, the W mediation dominates, and $f\bar{f}'$ are distributed with branching fractions similar to W decay products (barring phase space effects for small mass gaps between $\tilde{\chi}^\pm$ and $\tilde{\chi}^0$). If, on the other hand, sleptons are light enough to play a significant role in the decay mediation, leptonic final states will be enhanced.

At LEP, charginos have been searched for in fully-hadronic, semi-leptonic and fully leptonic decay modes [108,109]. A general lower limit on the lightest chargino mass of 103.5 GeV is derived, except in corners of phase space with low electron sneutrino mass, where destructive interference in chargino production, or two-body decay modes, play a role. The limit is also affected if the mass difference between $\tilde{\chi}_1^\pm$ and $\tilde{\chi}_1^0$ is

small; dedicated searches for such scenarios set a lower limit of 92 GeV.

At the Tevatron, charginos have been searched for via associated production of $\tilde{\chi}_1^{\pm}\tilde{\chi}_2^0$ [110,111]. Decay modes involving multilepton final states provide the best discrimination against the large multijet background. Analyses have looked for at least three charged isolated leptons, for two leptons with missing transverse momentum, or for two leptons with the same charge. Depending on the $(\tilde{\chi}_1^{\pm} - \tilde{\chi}_1^0)$ and/or $(\tilde{\chi}_2^0 - \tilde{\chi}_1^0)$ mass differences, leptons may be soft.

At the LHC, the search strategy is similar to that at the Tevatron. As shown in Fig. 1, the cross section of pair production of chargino and neutralinos at the LHC, for masses of several hundreds of GeV, is at least two orders of magnitude smaller than for colored SUSY particles (e.g. top squark pair production). For this reason a high statistics data sample is required to improve the sensitivity of LEP and Tevatron searches for direct chargino/neutralino production. With the full LHC Run 1 data, ATLAS and CMS have started to surpass the limits from LEP and Tevatron in regions of SUSY parameter space.

Chargino pair production is searched for in the dilepton plus missing momentum final state. In the simplified model interpretation of the results, assuming mediation of the chargino decay by light sleptons, ATLAS [112] and CMS [113] set limits on the chargino mass up to 540 GeV for massless LSPs, but no limits on the chargino mass can be set for $\tilde{\chi}_1^0$ heavier than 180 GeV. Limits are fairly robust against variation of the slepton mass, unless the mass gap between chargino and slepton becomes small. First limits are also set on charginos decaying via a W boson [114]: chargino masses below 180 GeV are excluded for massless LSPs, but no limits are set for LSPs heavier than 25 GeV. The trilepton plus missing momentum final state is used to set limits on $\tilde{\chi}_1^{\pm}\tilde{\chi}_2^0$ production, assuming wino-like $\tilde{\chi}^{\pm}$ and $\tilde{\chi}_2^0$, bino-like $\tilde{\chi}_1^0$, and $m_{\tilde{\chi}^{\pm}} = m_{\tilde{\chi}_2^0}$, leaving $m_{\tilde{\chi}^{\pm}}$ and $m_{\tilde{\chi}_1^0}$ free. Again, the branching fraction of leptonic final states is determined by the slepton masses. If the decay is predominantly mediated by a light $\tilde{\ell}_{\mathrm{L}}$, i.e. $\tilde{\ell}_{\mathrm{R}}$ is assumed to be heavy, the three lepton flavors will be produced in

equal amounts. It is assumed that $\tilde{\ell}_{\mathrm{L}}$ and sneutrino masses are equal, and diagrams with sneutrinos are included. In this scenario, ATLAS [112] and CMS [113] exclude chargino masses below 730 GeV for massless LSPs; no limits are set for LSP masses above 400 GeV. If the decay is dominated by a light $\tilde{\ell}_{\mathrm{R}}$, the chargino cannot be a pure wino but needs to have a large higgsino component, preferring the decays to tau leptons. Limits are set in various scenarios. If, like for $\tilde{\ell}_{\mathrm{L}}$, a flavor-democratic scenario is assumed, CMS sets limits of 620 GeV on the chargino mass for massless LSPs, but under the assumption that both $\tilde{\chi}^{\pm}$ and $\tilde{\chi}^0_2$ decay leads to tau leptons in the final state, the chargino mass limit deteriorates to 350 GeV for massless LSPs [113]. ATLAS assumes a simplified model in which staus are significantly lighter than the other sleptons in order to search for a similar multi-tau final state, and sets a similar limit on the chargino mass [112].

If sleptons are heavy, the chargino is assumed to decay to a W boson plus LSP, and the $\tilde{\chi}^0_2$ into Z plus LSP or H plus LSP. In the WZ channel, ATLAS [112] and CMS [113] limits on the chargino mass reach 420 GeV for massless LSPs, but no limits are set for LSPs heavier than 150 GeV. In the WH channel, for $m_H = 125$ GeV and using Higgs decays to $b\bar{b}$, $\gamma\gamma$ and WW (ATLAS [115]) , or Higgs decays to $b\bar{b}$, $\gamma\gamma$, WW, ZZ and $\tau^+\tau^-$ (CMS [113,116]) , assuming a SM-like branching fraction in these final states, chargino mass limits extend up to 250 GeV for massless LSPs, but vanish for LSPs above 40 GeV.

The CMS results on electroweak gaugino searches interpreted in simplified models are summarized in Fig. 8, the ATLAS results are similar.

In both the wino region (a characteristic of anomaly-mediated SUSY breaking models) and the higgsino region of the MSSM, the mass splitting between $\tilde{\chi}^{\pm}_1$ and $\tilde{\chi}^0_1$ is small. The chargino decay products are very soft and may escape detection. These compressed spectra are very hard to find, and have triggered dedicated search strategies, which, however, still have limited sensitivity. Photons or jets from initial state radiation may be used to tag such decays. An alternative production

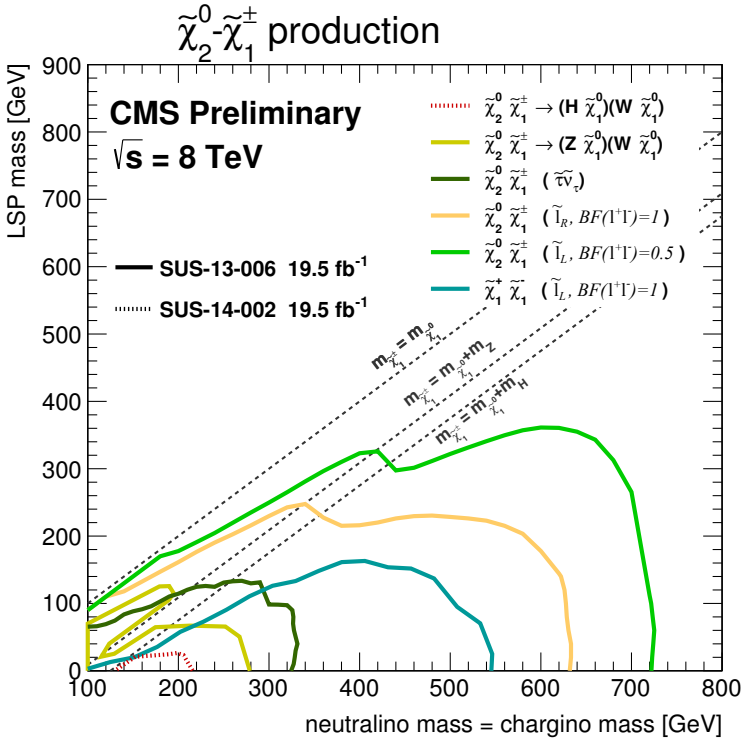

Figure 8: A summary of limits on chargino and neutralino masses in simplified models as obtained by CMS [158].

mode of electroweak gauginos is provided by vector-boson-fusion, where two additional jets with a large rapidity gap can be used to select events and suppress backgrounds [112,117].

In scenarios with compressed spectra, charginos may be long-lived. Charginos decaying in the detectors away from the primary vertex could lead to signatures such as kinked-tracks, or apparently disappearing tracks, since, for example, the pion in $\tilde{\chi}_1^\pm \rightarrow \pi^\pm \tilde{\chi}_1^0$ might be too soft to be reconstructed. At the LHC, searches have been performed for such disappearing tracks, and interpreted within anomaly-mediated SUSY breaking models [118,119]. Charginos with lifetimes between 0.1 and 10 ns are excluded for chargino masses up to 500 GeV. Within AMSB models, a lower limit on the chargino mass of 270 GeV is set, for a mass difference with the LSP of 160 MeV and a lifetime of 0.2 ns.

Charginos with a lifetime longer than the time needed to pass through the detector appear as charged stable massive particles. Limits have been derived by the LEP experiments [120], by D0 at the Tevatron [107], and by the LHC experiments [72,121,122]. For lifetimes above 100 ns, charginos below some 800 GeV are excluded.

II.5.2. Exclusion limits on neutralino masses

In a considerable part of the MSSM parameter space, and in particular when demanding that the LSP carries no electric or color charge, the lightest neutralino $\tilde{\chi}_1^0$ is the LSP. If R-parity is conserved, such a $\tilde{\chi}_1^0$ is stable. Since it is weakly interacting, it will typically escape detectors unseen. Limits on the invisible width of the Z boson apply to neutralinos with a mass below 45.5 GeV, but depend on the Z-neutralino coupling. Such a coupling could be small or even absent; in such a scenario there is no general lower limit on the mass of the lightest neutralino [123]. In models with gaugino mass unification and sfermion mass unification at the GUT scale, a lower limit on the neutralino mass is derived from limits from direct searches, notably for charginos and sleptons, and amounts to 47 GeV [124]. Assuming a constraining model like the CMSSM, this limit increases to 50 GeV at LEP; however the strong constraints now set by the LHC increase such CMSSM-derived $\tilde{\chi}_1^0$ mass limits to well above 200 GeV [125].

In gauge-mediated models, the LSP is typically a gravitino, and the phenomenology is determined by the nature of the next-to-lightest supersymmetric particle (NLSP). A NLSP neutralino will decay to a gravitino and a SM particle whose nature is determined by the neutralino composition. Final states with two high p_{T} photons and missing momentum are searched for, and interpreted in gauge mediation models with bino-like neutralinos [126–130].

Assuming the production of at least two neutralinos per event, neutralinos with large non-bino components can also be searched for by their decay in final states with missing momentum plus any two bosons out of the collection γ, Z, H. A number of searches at the LHC have tried to cover the rich phenomenology of the various Z and H decay modes [113,116,129–131].

In gauge mediation models, NLSP neutralino decays need not be prompt, and experiments have searched for late decays with photons in the final state. CDF have searched for delayed $\tilde{\chi}_1^0 \to \gamma\tilde{G}$ decays using the timing of photon signals in the calorimeter [132]. CMS has used the same technique at the LHC [133]. Results are given as upper limits on the neutralino production cross section as a function of neutralino mass and lifetime. D0 has looked at the direction of showers in the electromagnetic calorimeter with a similar goal [134], and ATLAS has searched for photon candidates that do not point back to the primary vertex, as well as for delayed photons [135].

Heavier neutralinos, in particular $\tilde{\chi}_2^0$, have been searched for in their decays to the lightest neutralino plus a γ, a Z boson or a Higgs boson. Limits on electroweak production of $\tilde{\chi}_2^0$ plus $\tilde{\chi}_1^\pm$ from trilepton analyses have been discussed in the section on charginos; the assumption of equal mass of $\tilde{\chi}_2^0$ and $\tilde{\chi}_1^\pm$ make the limits on chargino masses apply to $\tilde{\chi}_2^0$ as well. Multilepton analyses have also been used to set limits on $\tilde{\chi}_2^0\tilde{\chi}_3^0$ production; assuming equal mass limits are set up to 680 GeV for massless LSPs [112]. Again, compressed spectra with small mass differences between the heavier neutralinos and the LSP form the most challenging region.

In $\tilde{\chi}_2^0$ decays to $\tilde{\chi}_1^0$ and a lepton pair, the lepton pair invariant mass distribution may show a structure that can be used to measure the $\tilde{\chi}_2^0 - \tilde{\chi}_1^0$ mass difference in case of a signal [34]. This structure, however, can also be used in the search strategy itself, as demonstrated by CMS [136] and ATLAS [131].

In model with R-parity violation, the lightest neutralino can decay even if it is the lightest supersymmetric particle. If the decay involves a non-zero λ coupling, the final state will be a multi-lepton one. Searches for events with four or more isolated charged leptons by ATLAS [77,137] and CMS [78] are interpreted in such models. With very small coupling values, the neutralino would be long-lived, leading to lepton pairs with a displaced vertex, which have also been searched for [73,84]. Searches for events with a displaced hadronic vertex, with or without a matched lepton, are interpreted in a model with

R-parity violating neutralino decay involving a non-zero λ' coupling [73,138]. Neutralino decays involving non-zero λ'' lead to fully hadronic final states, and searches for jet-pair resonances are used to set limits, typically on the production of colored particles like top squarks or gluinos, which are assumed to be the primary produced sparticles in these interpretations, as discussed earlier.

Interpretations of the search results outside simplified models, such as in the phenomenological MSSM [139–141], show that the simplified model limits must be interpreted with care. Electroweak gauginos in models that are compatible with the relic density of dark matter in the universe, for example, have particularly tuned mixing parameters and mass spectra, which are not always captured by the simplified models used.

II.6. Exclusion limits on slepton masses

In models with slepton and gaugino mass unification at the GUT scale, the right-handed slepton, $\tilde{\ell}_{\mathrm{R}}$, is expected to be lighter than the left-handed slepton, $\tilde{\ell}_{\mathrm{L}}$. For tau sleptons there may be considerable mixing between the L and R states, leading to a significant mass difference between the lighter $\tilde{\tau}_1$ and the heavier $\tilde{\tau}_2$.

II.6.1. Exclusion limits on the masses of charged sleptons

The most model-independent searches for selectrons, smuons and staus originate from the LEP experiments [142]. Smuon production only takes place via s-channel γ^*/Z exchange. Search results are often quoted for $\tilde{\mu}_{\mathrm{R}}$, since it is typically lighter than $\tilde{\mu}_{\mathrm{L}}$ and has a weaker coupling to the Z boson; limits are therefore conservative. Decays are expected to be dominated by $\tilde{\mu}_{\mathrm{R}} \to \mu\tilde{\chi}_1^0$, leading to two non-back-to-back muons and missing momentum. Slepton mass limits are calculated in the MSSM under the assumption of gaugino mass unification at the GUT scale, and depend on the mass difference between the smuon and $\tilde{\chi}_1^0$. A $\tilde{\mu}_{\mathrm{R}}$ with a mass below 94 GeV is excluded for $m_{\tilde{\mu}_{\mathrm{R}}} - m_{\tilde{\chi}_1^0} > 10$ GeV. The selectron case is similar to the smuon case, except that an additional production mechanism is provided by t-channel neutralino exchange. The

Table 3: Summary of weak gaugino mass limits in simplified models, assuming R-parity conservation. Masses in the table are provided in GeV. Further details about assumptions and analyses from which these limits are obtained are discussed in the text.

Assumption	m_χ
$\tilde{\chi}_1^\pm$, all $\Delta m(\tilde{\chi}_1^\pm, \tilde{\chi}_1^0)$	> 92
$\tilde{\chi}_1^\pm$ $\Delta m > 5$, $m_{\tilde{\nu}} > 300$	> 103.5
$\tilde{\chi}_1^\pm$, $m_{(\tilde{\ell},\tilde{\nu})} = (m_{\tilde{\chi}_1^\pm} + m_{\tilde{\chi}_1^0})/2$	
$m_{\tilde{\chi}_1^0} \approx 0$	> 540
$\tilde{\chi}_1^\pm$, $m_{\tilde{\chi}_1^0} > 180$	no LHC limit
$\tilde{\chi}_1^\pm$, $m_{\tilde{\ell}} > m_{\tilde{\chi}_1^\pm}$	
$m_{\tilde{\chi}_1^0} \approx 0$	> 180
$\tilde{\chi}_1^\pm$, $m_{\tilde{\chi}_1^0} > 25$	no LHC limit
$m_{\tilde{\chi}_1^\pm} = m_{\tilde{\chi}_2^0}$, $m_{\tilde{\ell}_\mathrm{L}} = (m_{\tilde{\chi}_1^\pm} + m_{\tilde{\chi}_1^0})/2$	
$m_{\tilde{\chi}_1^0} \approx 0$	> 730
$m_{\tilde{\chi}_1^0} > 400$	no LHC limit
$m_{\tilde{\chi}_1^\pm} = m_{\tilde{\chi}_2^0}$, $m_{\tilde{\ell}_\mathrm{R}} = (m_{\tilde{\chi}_1^\pm} + m_{\tilde{\chi}_1^0})/2$	flavor-democratic
$m_{\tilde{\chi}_1^0} \approx 0$	> 620
$m_{\tilde{\chi}_1^0} > 220$	no LHC limit
$m_{\tilde{\chi}_1^\pm} = m_{\tilde{\chi}_2^0}$, $m_{\tilde{\tau}} = (m_{\tilde{\chi}_1^\pm} + m_{\tilde{\chi}_1^0})/2$	$\tilde{\tau}$-dominated
$m_{\tilde{\chi}_1^0} \approx 0$	> 350
$m_{\tilde{\chi}_1^0} > 120$	no LHC limit
$m_{\tilde{\chi}_1^\pm} = m_{\tilde{\chi}_2^0}$, $m_{\tilde{\ell}} > m_{\tilde{\chi}_1^\pm}$, $\mathrm{BF}(WZ) = 1$	
$m_{\tilde{\chi}_1^0} \approx 0$	> 420
$m_{\tilde{\chi}_1^0} > 150$	no LHC limit
$m_{\tilde{\chi}_1^\pm} = m_{\tilde{\chi}_2^0}$, $m_{\tilde{\ell}} > m_{\tilde{\chi}_1^\pm}$, $\mathrm{BF}(WH) = 1$	
$m_{\tilde{\chi}_1^0} \approx 0$	> 250
$m_{\tilde{\chi}_1^0} > 40$	no LHC limit

$\tilde{e}_\mathrm{R}$ lower mass limit is 100 GeV for $m_{\tilde{\chi}_1^0} < 85$ GeV. Due to the t-channel neutralino exchange, $\tilde{e}_\mathrm{R}\tilde{e}_\mathrm{L}$ pair production was possible at LEP, and a lower limit of 73 GeV was set on the selectron mass regardless of the neutralino mass by scanning over MSSM

parameter space [143]. The potentially large mixing between $\tilde{\tau}_{\mathrm{L}}$ and $\tilde{\tau}_{\mathrm{R}}$ not only makes the $\tilde{\tau}_1$ light, but can also make its coupling to the Z boson small. LEP lower limits on the $\tilde{\tau}$ mass range between 87 and 93 GeV depending on the $\tilde{\chi}_1^0$ mass, for $m_{\tilde{\tau}} - m_{\tilde{\chi}_1^0} > 7$ GeV [142].

As shown in Fig. 1, at the LHC pair production of sleptons is not only heavily suppressed with respect to pair production of colored SUSY particles but the cross section is also almost two orders of magnitude smaller than the one of pair production of chargino and neutralinos. Only with the full Run 1 LHC data set, ATLAS and CMS have started to surpass the sensitivity of the LEP analyses under certain assumptions.

ATLAS and CMS have searched for direct production of selectron pairs and smuon pairs at the LHC, with each slepton decaying to its corresponding SM partner lepton and the $\tilde{\chi}_1^0$ LSP. ATLAS [114] and CMS [113] set limits in this model of 240 GeV for $\tilde{\ell}_{\mathrm{R}}$, and 290 GeV for $\tilde{\ell}_{\mathrm{L}}$, for a massless $\tilde{\chi}_1^0$ and assuming equal selectron and smuon masses, as shown in Fig. 9. The limits deteriorate with increasing $\tilde{\chi}_1^0$ mass due to decreasing missing momentum and lepton momentum. As a consequence, there is a gap between LEP and LHC limits for $\tilde{\chi}_1^0$ masses above 20 GeV, and no limits are set for $\tilde{\chi}_1^0$ masses above 90 GeV ($\tilde{\ell}_{\mathrm{R}}$) or above 150 GeV ($\tilde{\ell}_{\mathrm{L}}$).

In gauge-mediated SUSY breaking models, sleptons can be (co-)NLSPs, *i.e.*, the next-to-lightest SUSY particles and almost degenerate in mass, decaying to a lepton and a gravitino. This decay can either be prompt, or the slepton can have a non-zero lifetime. Combining several analyses, lower mass limits on $\tilde{\mu}_{\mathrm{R}}$ of 96.3 GeV and on $\tilde{e}_{\mathrm{R}}$ of 66 GeV are set for all slepton lifetimes at LEP [144]. In a considerable part of parameter space in these models, the $\tilde{\tau}$ is the NLSP. The LEP experiments have set lower limits on the mass of such a $\tilde{\tau}$ between 87 and 97 GeV, depending on the $\tilde{\tau}$ lifetime. ATLAS has searched for final states with τs, jets and missing transverse momentum, and has interpreted the results in GMSB models setting limits on the model parameters [145]. CMS has interpreted a multilepton analysis in terms of limits on gauge mediation models with slepton (co-)NLSP [146]. CDF has put

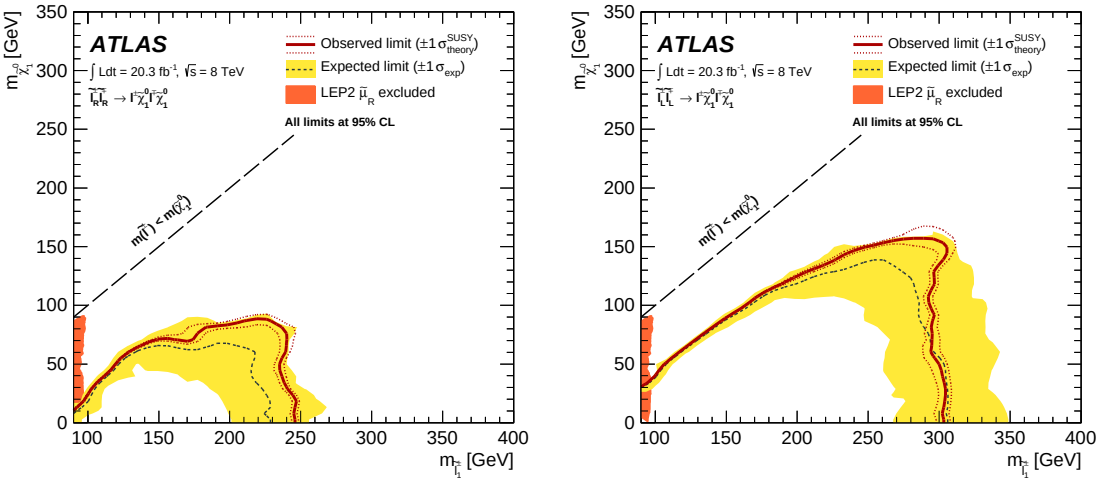

Figure 9: Exclusion limits on $\tilde{\ell}_{\mathrm{R}}$ masses (left) and $\tilde{\ell}_{\mathrm{L}}$ masses (right), assuming equal selectron and smuon masses in both scenarios, and assuming a 100% branching fraction for $\tilde{\ell} \to \ell\tilde{\chi}_1^0$ [114].

limits on gauge mediation models at high $\tan\beta$ and slepton (co-)NLSP using an analysis searching for like-charge light leptons and taus [147].

Limits also exist on sleptons in R-parity violating models, both from LEP and the Tevatron experiments. From LEP, lower limits on $\tilde{\mu}_{\mathrm{R}}$ and $\tilde{e}_{\mathrm{R}}$ masses in such models are 97 GeV, and the limits on the stau mass are very close: 96 GeV [148].

Charged slepton decays may be kinematically suppressed, for example in the scenario of a NLSP slepton with a very small mass difference to the LSP. Such a slepton may appear to be a stable charged massive particle. Interpretation of searches at LEP for such signatures within GMSB models with stau NLSP or slepton co-NLSP exclude masses up to 99 GeV [120]. Searches of stable charged particles at the Tevatron [106,107] and at the LHC [71,72] are also interpreted in terms of limits on stable charged sleptons. The limits obtained at the LHC exclude stable staus with masses below 339 GeV when produced directly in pairs, and below 500 GeV when staus are produced both directly and indirectly in the decay of other particles in a GMSB model.

II.6.2. Exclusion limits on sneutrino masses

The invisible width of the Z boson puts a lower limit on the sneutrino mass of about 45 GeV. Tighter limits are derived from other searches, notably for gauginos and sleptons, under the assumption of gaugino and sfermion mass universality at the GUT scale, and amount to approximately 94 GeV in the MSSM [149]. It is possible that the lightest sneutrino is the LSP; however, a left-handed sneutrino LSP is ruled out as a cold dark matter candidate [150,151].

Production of pairs of sneutrinos in R-parity violating models has been searched for at LEP [148]. Assuming fully leptonic decays via λ-type couplings, lower mass limits between 85 and 100 GeV are set. At the Tevatron [152,153] and at the LHC [154,155], searches have focused on scenarios with resonant production of a sneutrino, decaying to $e\mu$, $\mu\tau$ and $e\tau$ final states. No signal has been seen, and limits have been set on sneutrino masses as a function of the value of relevant RPV couplings. As an example, the LHC experiments exclude a resonant tau sneutrino with a mass below 1500 GeV for $\lambda_{312} > 0.07$ and $\lambda'_{311} > 0.01$.

Table 4: Summary of slepton mass limits from LEP and LHC, assuming R-parity conservation and 100% branching fraction for $\tilde{\ell} \to \ell\tilde{\chi}_1^0$. Masses in this table are provided in GeV.

Assumption	$m_{\tilde{\ell}}$
$\tilde{\mu}_{\rm R}$, $\Delta m(\tilde{\mu}_{\rm R}, \tilde{\chi}_1^0) > 10$	> 94
$\tilde{e}_{\rm R}$, $\Delta m(\tilde{e}_{\rm R}, \tilde{\chi}_1^0) > 10$	> 94
$\tilde{e}_{\rm R}$, any Δm	> 73
$\tilde{\tau}_{\rm R}$, $\Delta m((\tilde{\tau}_{\rm R}, \tilde{\chi}_1^0) > 7$	> 87
$\tilde{\nu}_e$, $\Delta m(\tilde{e}_{\rm R}, \tilde{\chi}_1^0) > 10$	> 94
$m_{\tilde{e}_{\rm R}} = m_{\tilde{\mu}_{\rm R}}$, $m_{\tilde{\chi}_1^0} \approx 0$	> 240
$m_{\tilde{\chi}_1^0} >\approx 90$	no LHC limit
$m_{\tilde{e}_{\rm L}} = m_{\tilde{\mu}_{\rm L}}$, $m_{\tilde{\chi}_1^0} \approx 0$	> 290
$m_{\tilde{\chi}_1^0} >\approx 150$	no LHC limit

II.7. Global interpretations

Apart from the interpretation of direct searches for sparticle production at colliders in terms of limits on masses of individual SUSY particles, model-dependent interpretations of allowed SUSY parameter space are derived from global SUSY fits. Typically these fits combine the results from collider experiments with indirect constraints on SUSY as obtained from low-energy experiments, flavor physics, high-precision electroweak results, and astrophysical data.

In the pre-LHC era these fits were mainly dominated by indirect constraints. Even for very constrained models like the CMSSM, the allowed parameter space, in terms of squark and gluino masses, ranged from several hundreds of GeV to a few TeV. Furthermore, these global fits indicated that squarks and gluino masses in the range of 500 to 1000 GeV were the preferred region of parameter space, although values as high as few TeV were allowed with lower probabilities [156].

With ATLAS and CMS now probing mass scales around 1 TeV and even beyond, the importance of the direct searches for global analyses of allowed SUSY parameter space has strongly increased. For example, imposing the new experimental limits on constrained supergravity models pushes the most likely values of first generation squark and gluino masses significantly beyond 1 TeV, typically resulting in overall values of fit quality much worse than those in the pre-LHC era [125]. Although these constrained models are not yet ruled out, the extended experimental limits impose tight constraints on the allowed parameter space.

For this reason, the emphasis of global SUSY fits has shifted towards less-constrained SUSY models. Especially interpretations in the pMSSM [121,139–141] but also in simplified models have been useful to generalize SUSY searches, for example to redesign experimental analyses in order to increase their sensitivity for compressed spectra, where the mass of the LSP is much closer to squark and gluino masses than predicted, for example, by the CMSSM. As shown in Table 2, for neutralino masses above a few hundred GeV the current set of ATLAS and CMS searches cannot exclude the existence of light squarks

and also gluinos above approximately 1 TeV are not yet fully excluded.

Furthermore, the discovery of a Higgs boson with a mass around 125 GeV has triggered many studies regarding the compatibility of SUSY parameter space with this new particle. Much of it is still work in progress and it will be interesting to see how the interplay between the results from direct SUSY searches and more precise measurements of the properties of the Higgs boson will unfold in the forthcoming era of high-energy running of the LHC.

II.8. Summary and Outlook

Direct searches for SUSY, combined with limits from high-precision experiments that look for new physics in loops, put SUSY under considerable scrutiny. In particular the absence of any observation of new phenomena at the first run of the LHC, at $\sqrt{s} = 7$ and 8 TeV, place significant constraints on SUSY parameter space. Today, inclusive searches probe production of gluinos in the rage of $1.0 - 1.4$ TeV, first and second generation squarks to about 1.0 TeV , third generation squarks at scales around 600 GeV, electroweak gauginos at scales around $300 - 500$ GeV, and sleptons around 200 GeV. However, depending on the assumptions made of the underlying SUSY spectrum these limits can also weaken considerably. An overview of the current landscape of SUSY searches and corresponding exclusion limits at the LHC is shown in Fig. 10 from the ATLAS experiment [157]. The corresponding results of the CMS experiment are similar [158].

The interpretation of results at the LHC has moved away from constrained models like the CMSSM towards a large set of simplified models, or the pMSSM. On the one hand this move is because the LHC limits have put constrained models like the CMSSM under severe pressure, while on the other hand simplified models leave more freedom to vary parameters and form a better representation of the underlying sensitivity of analyses. However, these interpretations in simplified models do not come without a price: the decomposition of a potentially complicated reality in a limited set of individual decay chains can be significantly incomplete. Therefore, quoted limits in simplified

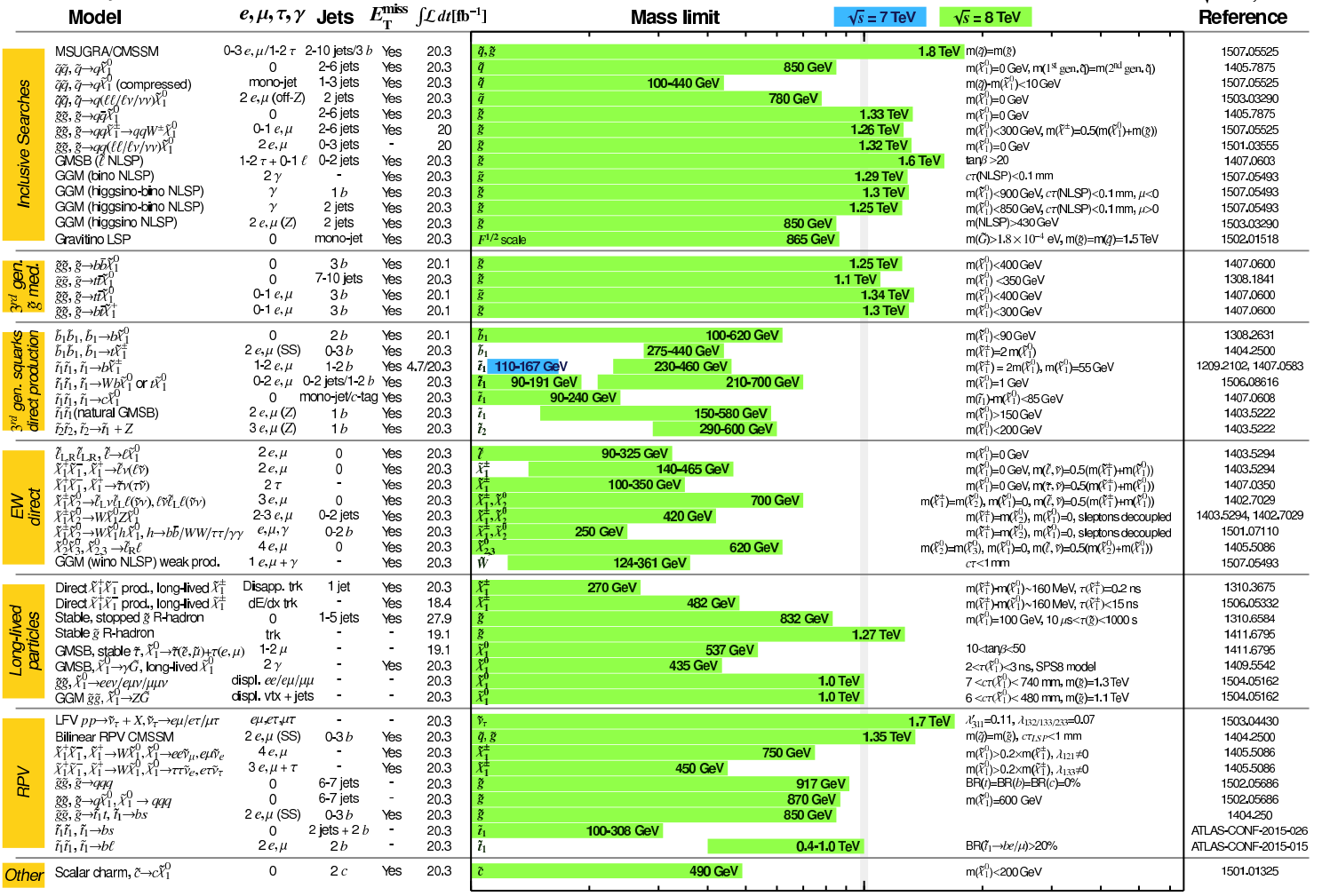

*Only a selection of the available mass limits on new states or phenomena is shown. All limits quoted are observed minus 1σ theoretical signal cross section uncertainty.

Figure 10: Overview of the current landscape of SUSY searches at the LHC. The plot shows exclusion mass limits of ATLAS for different searches and interpretation assumptions [157]. The corresponding results of CMS are comparable.

February 8, 2016 19:57

models are only valid under the explicit assumptions made in these models, assumptions that are usually stated on the plots, and in the relevant LHC papers. Interpretations of simplified models in generic cases, ignoring the assumptions made, can lead to overestimation of limits on SUSY parameter space. The recent addition of more comprehensive interpretations in the pMSSM is expected to overcome some of the limitations arising from the characterisation of searches in simplified model and thus will enable an even more refined understanding of the probed SUSY parameter space. In this context, the limit range of $1.0 - 1.4$ TeV on generic colored SUSY particles only holds for light neutralinos, in the R-parity conserving MSSM. Limits on third generation squarks and electroweak gauginos also only hold for light neutralinos, and under specific assumptions for decay modes and slepton masses. In general, SUSY below the 1 TeV scale is not yet ruled out.

The new LHC run at $\sqrt{s} = 13$ TeV, with significantly larger integrated luminosities, will present again a great opportunity for SUSY searches. The operation at higher energy will increase the production cross section for SUSY particles, shown in Fig. 1, substantially. While typically for masses around 500 GeV the increase is about 3 to 5 times the production cross section at 8 TeV, this becomes an increase of almost two orders of magnitude for a SUSY mass scale of 1.5 to 2 TeV. Apart from pushing the sensitivity of LHC searches to higher mass scales, further LHC data will also help to reduce holes and gaps that are left behind in today's SUSY limits. These could be, for example, due to compressed particle spectra, stealth SUSY, or the violation of R-parity.

References

1. H. Miyazawa, Prog. Theor. Phys. **36**, 1266 (1966).
2. Yu. A. Golfand and E.P. Likhtman, Sov. Phys. JETP Lett. **13**, 323 (1971).
3. J.L. Gervais and B. Sakita, Nucl. Phys. **B34**, 632 (1971).
4. D.V. Volkov and V.P. Akulov, Phys. Lett. **B46**, 109 (1973).
5. J. Wess and B. Zumino, Phys. Lett. **B49**, 52 (1974).
6. J. Wess and B. Zumino, Nucl. Phys. **B70**, 39 (1974).

7. A. Salam and J.A. Strathdee, Nucl. Phys. **B76**, 477 (1974).
8. H.P. Nilles, Phys. Reports **110**, 1 (1984).
9. H.E. Haber and G.L. Kane, Phys. Reports **117**, 75 (1987).
10. E. Witten, Nucl. Phys. **B188**, 513 (1981).
11. S. Dimopoulos and H. Georgi, Nucl. Phys. **B193**, 150 (1981).
12. M. Dine, W. Fischler, and M. Srednicki, Nucl. Phys. **B189**, 575 (1981).
13. S. Dimopoulos and S. Raby, Nucl. Phys. **B192**, 353 (1981).
14. N. Sakai, Z. Phys. **C11**, 153 (1981).
15. R.K. Kaul and P. Majumdar, Nucl. Phys. **B199**, 36 (1982).
16. H. Goldberg, Phys. Rev. Lett. **50**, 1419 (1983).
17. J.R. Ellis *et al.*, Nucl. Phys. **B238**, 453 (1984).
18. G. Jungman and M. Kamionkowski, Phys. Reports **267**, 195 (1996).
19. S. Dimopoulos, S. Raby, and F. Wilczek, Phys. Rev. **D24**, 1681 (1981).
20. W.J. Marciano and G. Senjanović, Phys. Rev. **D25**, 3092 (1982).
21. M.B. Einhorn and D.R.T. Jones, Nucl. Phys. **B196**, 475 (1982).
22. L.E. Ibanez and G.G. Ross, Phys. Lett. **B105**, 439 (1981).
23. N. Sakai, Z. Phys. **C11**, 153 (1981).
24. U. Amaldi, W. de Boer, and H. Furstenau, Phys. Lett. **B260**, 447 (1991).
25. P. Langacker and N. Polonsky, Phys. Rev. **D52**, 3081 (1995).
26. P. Fayet, Phys. Lett. **B64**, 159 (1976).
27. G.R. Farrar and P. Fayet, Phys. Lett. **B76**, 575 (1978).
28. H.E. Haber, *Supersymmetry, Part I (Theory)*, in this *Review*.
29. CMS Collab. and LHCb Collab., Nature **522**, 68 (2015).
30. G. Hinshaw *et al.*, Astrophys. J. Supp. **208**, 19H (2013).
31. Planck Collab, *Planck 2015 results. XIII. Cosmological parameters*, `arXiv:1502.01589 [astro-ph.CO]`.
32. M. Carena *et al.*, *Higgs Bosons: Theory and Searches*, this *Review*.

33. J.F. Grivaz, *Supersymmetry, Part II (Experiment)*, in: 2010 Review of Particle Physics, K. Nakamura *et al.*, (Particle Data Group), J. Phys. **G37**, 075021 (2010).
34. I. Hinchliffe *et al.*, Phys. Rev. **D55**, 5520 (1997).
35. L. Randall and D. Tucker-Smith, Phys. Rev. Lett. **101**, 221803 (2008).
36. CMS Collab., Phys. Lett. **B698**, 196 (2011).
37. CMS Collab., Phys. Rev. Lett. **107**, 221804 (2011).
38. CMS Collab., JHEP **1301**, 077 (2013).
39. CMS Collab., Eur. Phys. J. **C73**, 2568 (2013).
40. CMS Collab., Phys. Rev. **D85**, 012004 (2012).
41. C.G. Lester and D.J. Summers, Phys. Lett. **B463**, 99 (1999).
42. D.R. Tovey, JHEP **0804**, 034 (2008).
43. A.H. Chamseddine, R. Arnowitt, and P Nath, Phys. Rev. Lett. **49**, 970 (1982).
44. E. Cremmer *et al.*, Nucl. Phys. **B212**, 413 (1983).
45. P. Fayet, Phys. Lett. **B70**, 461 (1977).
46. M. Dine, A.E. Nelson, and Yu. Shirman, Phys. Rev. **D51**, 1362 (1995).
47. G.F. Giudice *et al.*, JHEP **9812**, 027 (1998).
48. L. Randall and R. Sundrum, Nucl. Phys. **B557**, 79 (1999).
49. R. Arnowitt and P Nath, Phys. Rev. Lett. **69**, 725 (1992).
50. G.L. Kane *et al.*, Phys. Rev. **D49**, 6173 (1994).
51. P. Meade, N. Seiberg, and D. Shih, Prog. Theor. Phys. Supp. **177**, 143 (2009).
52. W. Beenakker *et al.*, Nucl. Phys. **B492**, 51 (1997); W. Beenakker *et al.*, Nucl. Phys. **B515**, 3 (1998); W. Beenakker *et al.*, Phys. Rev. Lett. **83**, 3780 (1999), Erratum *ibid.*, **100**, 029901 (2008); M. Spira, `hep-ph/0211145 (2002)`; T. Plehn, Czech. J. Phys. 55, B213 (2005).
53. A. Djouadi, J-L. Kneur, and G. Moultaka, Comp. Phys. Comm. **176**, 426 (2007).
54. C.F. Berger *et al.*, JHEP **0902**, 023 (2009).
55. H. Baer *et al.*, `hep-ph/9305342`, 1993.
56. R.M. Barnett, H.E. Haber, and G.L. Kane, Nucl. Phys. **B267**, 625 (1986).
57. H. Baer, D. Karatas, and X. Tata, Phys. Lett. **B183**, 220 (1987).

58. J. Alwall, Ph.C. Schuster, and N. Toro, Phys. Rev. **D79**, 075020 (2009).
59. J. Alwall *et al.*, Phys. Rev. **D79**, 015005 (2009).
60. O. Buchmueller and J. Marrouche, Int. J. Mod. Phys. **A29**, 1450032 (2014).
61. LEP2 SUSY Working Group, ALEPH, DELPHI, L3 and OPAL experiments, note LEPSUSYWG/04-02.1, `http://lepsusy.web.cern.ch/lepsusy`.
62. ATLAS Collab., JHEP **1510**, 054 (2015).
63. CDF Collab., Phys. Rev. Lett. **102**, 121801 (2009).
64. D0 Collab., Phys. Lett. **B660**, 449 (2008).
65. CMS Collab., JHEP **1505**, 078 (2015).
66. CMS Collab., Phys. Lett. **B725**, 243 (2013).
67. CMS Collab., Eur. Phys. J. **C73**, 2568 (2013).
68. CMS Collab,. Phys. Rev. **D91**, 052018 (2015).
69. ATLAS Collab., JHEP **1410**, 24 (2014).
70. CMS Collab., Phys. Lett. **B733**, 328 (2014).
71. CMS Collab., JHEP **1307**, 122 (2013).
72. ATLAS Collab., JHEP **1501**, 068 (2015).
73. ATLAS Collab., Phys. Rev. **D92**, 072004 (2015).
74. D0 Collab., Phys. Rev. Lett. **99**, 131801 (2007).
75. ATLAS Collab., Phys. Rev. **D88**, 112003 (2013).
76. CMS Collab., Eur. Phys. J. **C75**, 151 (2015).
77. ATLAS Collab., *Constraints on promptly decaying supersymmetric particles with lepton-number- and R-parity-violating interactions using Run-1 ATLAS data*, ATLAS-CONF-2015-018 (2015).
78. CMS Collab., *Search for RPV SUSY in the four-lepton final state*, CMS-PAS-SUS-13-010 (2013).
79. CDF Collab., Phys. Rev. Lett. **107**, 042001 (2011).
80. ATLAS Collab., Phys. Rev. **D91**, 112016 (2015).
81. CMS Collab., Phys. Lett. **B730**, 193 (2014).
82. ATLAS Collab,. Phys. Rev. Lett. **114**, 161801 (2015).
83. H1 Collab., Eur. Phys. J. **C71**, 1572 (2011).
84. CMS Collab., Phys. Rev. **D91**, 052012 (2015).
85. ATLAS Collab., Eur. Phys. J. **C75**, 510 (2015).
86. CDF Collab., Phys. Rev. Lett. **105**, 081802 (2010).
87. D0 Collab., Phys. Lett. **B693**, 95 (2010).
88. CMS Collab., JHEP **1506**, 116 (2015).

89. CMS Collab., JHEP **1303**, 037 (2013), JHEP **1307**, 041 (2013).
90. C. Boehm, A. Djouadi, and Y. Mambrini, Phys. Rev. **D61**, 095006 (2000).
91. CDF Collab., Phys. Rev. **D82**, 092001 (2010).
92. D0 Collab., Phys. Lett. **B696**, 321 (2011).
93. CDF Collab., JHEP **1210**, 158 (2012).
94. D0 Collab., Phys. Lett. **B665**, 1 (2008).
95. CDF Collab., Phys. Rev. Lett. **104**, 251801 (2010).
96. D0 Collab., Phys. Lett. **B674**, 4 (2009).
97. ATLAS Collab., JHEP **1509**, 015 (2014).
98. ATLAS Collab., JHEP **1411**, 118 (2014).
99. CMS Collab., Eur. Phys. J. **C73**, 2667 (2013).
100. ZEUS Collab., Eur. Phys. J. **C50**, 269 (2007).
101. CMS Collab., Phys. Rev. Lett. **111**, 221801 (2013).
102. ATLAS Collab., *A search for $B-L$ R-parity-violating scalar top decays in $\sqrt{s}=8$ TeV pp collisions with the ATLAS experiment*, ATLAS-CONF-2015-015 (2015).
103. CMS Collab., Phys. Rev. Lett. **114**, 061801 (2015).
104. ATLAS Collab., *A search for R-parity-violating scalar top decays in all-hadronic final states with the ATLAS detector in $\sqrt{s}=8$ TeV pp collisions*, ATLAS-CONF-2015-026 (2015).
105. CMS Collab., Phys. Lett. **B747**, 98 (2015).
106. CDF Collab., Phys. Rev. Lett. **103**, 021802 (2009).
107. D0 Collab., Phys. Rev. **D87**, 052011 (2013).
108. LEP2 SUSY Working Group, ALEPH, DELPHI, L3 and OPAL experiments, note LEPSUSYWG/01-03.1, `http://lepsusy.web.cern.ch/lepsusy`.
109. LEP2 SUSY Working Group, ALEPH, DELPHI, L3 and OPAL experiments, note LEPSUSYWG/02-04.1, `http://lepsusy.web.cern.ch/lepsusy`.
110. CDF Collab., *Search for trilepton new physics and chargino-neutralino production at the Collider Detector at Fermilab*, CDF Note 10636 (2011).
111. D0 Collab., Phys. Lett. **B680**, 34 (2009).
112. ATLAS Collab., *Search for the electroweak production of supersymmetric particles in $\sqrt{s}=8$ TeV pp collisions with the ATLAS detector*, `arXiv:1509.07152`(2015).
113. CMS Collab., Eur. Phys. J. **C74**, 3036 (2014).
114. ATLAS Collab., JHEP **1405**, 071 (2014).

115. ATLAS Collab., Eur. Phys. J. **C75**, 208 (2015).
116. CMS Collab., Phys. Rev. **D90**, 092007 (2014).
117. CMS Collab., *Search for supersymmetry in the vector-boson fusion topology in proton-proton collisions at* $\sqrt{s}$ *=8 TeV*, `arXiv:1508.07628`(2015).
118. ATLAS Collab., Phys. Rev. **D88**, 112006 (2013).
119. CMS Collab., JHEP **1501**, 096 (2015).
120. LEP2 SUSY Working Group, ALEPH, DELPHI, L3 and OPAL experiments, note LEPSUSYWG/02-05.1, `http://lepsusy.web.cern.ch/lepsusy`.
121. CMS Collab., Eur. Phys. J. **C75**, 325 (2015).
122. LHCb Collab., *Search for long-lived heavy charged particles using a ring imaging Cherenkov technique at LHCb*, `arXiv:1506.09173` (2015).
123. H. Dreiner *et al.*, Eur. Phys. J. **C62**, 547 (2009).
124. LEP2 SUSY Working Group, ALEPH, DELPHI, L3 and OPAL experiments, note LEPSUSYWG/04-07.1, `http://lepsusy.web.cern.ch/lepsusy`.
125. For a sampling of recent post-LHC global analyses, see: P. Bechtle *et al.*, `arXiv:1508.05951` (2015), O. Buchmueller *et al.*, Eur. Phys. J. **C74**, 3212 (2014); O. Buchmueller *et al.*, Eur. Phys. J. **C74**, 2922 (2014); M. Citron *et al.*, Phys. Rev. **D87**, 036012 (2013); C. Strege *et al.*, JCAP **1304**, 013 (2013); A. Fowlie *et al.*, Phys. Rev. **D86**, 075010 (2012).
126. LEP2 SUSY Working Group, ALEPH, DELPHI, L3 and OPAL experiments, note LEPSUSYWG/04-09.1, `http://lepsusy.web.cern.ch/lepsusy`.
127. CDF Collab., Phys. Rev. Lett. **104**, 011801 (2010).
128. D0 Collab., Phys. Rev. Lett. **105**, 221802 (2010).
129. ATLAS Collab., Phys. Rev. **D92**, 072001 (2015).
130. CMS Collab., Phys. Rev. **D92**, 072006 (2015).
131. ATLAS Collab., Eur. Phys. J. **C75**, 318 (2015).
132. CDF Collab., Phys. Rev. **D88**, 031103 (2013).
133. CMS Collab., Phys. Lett. **B722**, 273 (2013).
134. D0 Collab., Phys. Rev. Lett. **101**, 111802 (2008).
135. ATLAS Collab, Phys. Rev. **D90**, 112005 (2014).
136. CMS Collab., *Search for physics beyond the standard model in events with two opposite-sign same-flavor leptons, jets, and missing transverse energy in pp collisions at* $\sqrt{s}$ *= 8 TeV*, CMS-PAS-SUS-12-019 (2014).
137. ATLAS Collab., Phys. Rev. **D90**, 052001 (2014).

138. CMS Collab., Phys. Rev. **D91**, 012007 (2015).
139. ATLAS Collab., JHEP **1510**, 134 (2015).
140. CMS Collab., *Phenomenological MSSM interpretation of the CMS 7 and 8 TeV results*, CMS-PAS-SUS-13-020 (2014), CMS-PAS-SUS-15-010 (2015).
141. For a sampling of recent pMSSM analyses, see: K. de Vries *et al.*, Eur. Phys. J. **C75**, 422 (2015); C. Strege *et al.*, JHEP **1409**, 081 (2014); M. Cahill-Rowley *et al.*, Phys. Rev. **D88**, 035002 (2013); C. Boehm *et al.*, JHEP **1306**, 113, (2013); S AbdusSalam, Phys. Rev. **D87**, 115012 (2013); A. Arbey *et al.*, Eur. Phys. J. **C72**, 2169 (2012); A. Arbey *et al.*, Eur. Phys. J. **C72**, 1847 (2012); M. Carena *et al.*, Phys. Rev. **D86**, 075025 (2012); S. Sekmen *et al.*, JHEP **1202**, 075 (2012).
142. LEP2 SUSY Working Group, ALEPH, DELPHI, L3 and OPAL experiments, note LEPSUSYWG/04-01.1, `http://lepsusy.web.cern.ch/lepsusy`.
143. ALEPH Collab., Phys. Lett. **B544**, 73 (2002).
144. LEP2 SUSY Working Group, ALEPH, DELPHI, L3 and OPAL experiments, note LEPSUSYWG/02-09.2, `http://lepsusy.web.cern.ch/lepsusy`.
145. ATLAS Collab., JHEP **1409**, 103 (2014).
146. CMS Collab., Phys. Rev. **D90**, 032006 (2014).
147. CDF Collab., Phys. Rev. Lett. **110**, 201802 (2013).
148. LEP2 SUSY Working Group, ALEPH, DELPHI, L3 and OPAL experiments, note LEPSUSYWG/02-10.1, `http://lepsusy.web.cern.ch/lepsusy`.
149. DELPHI Collab., Eur. Phys. J. **C31**, 412 (2003).
150. T. Falk, K.A. Olive, and M. Srednicki, Phys. Lett. **B339**, 248 (1994).
151. C. Arina and N. Fornengo, JHEP **0711**, 029 (2007).
152. CDF Collab., Phys. Rev. Lett. **105**, 191801 (2010).
153. D0 Collab., Phys. Rev. Lett. **105**, 191802 (2010).
154. ATLAS Collab., Phys. Rev. Lett. **115**, 031801 (2015).
155. CMS Collab., *Search for Lepton Flavour Violating Decays of Heavy Resonances and Quantum Black Holes to electron/muon Pairs in pp Collisions at a centre of mass energy of 8 TeV*, CMS-PAS-EXO-13-002 (2015).
156. For a sampling of pre-LHC global analyses, see: O. Buchmueller *et al.*, Eur. Phys. J. **C71**, 1722 (2011); E.A. Baltz and P. Gondolo, JHEP **0410**, 052 (2004); B.C. Allanach and C.G. Lester, Phys. Rev. **D73**, 015013 (2006); R.R. de Austri *et al.*, JHEP **0605**, 002 (2006); R. Lafaye *et al.*,

Eur. Phys. J. **C54**, 617 (2008); S. Heinemeyer *et al.*, JHEP **0808**, 08 (2008); R. Trotta *et al.*, JHEP **0812**, 024 (2008); P. Bechtle *et al.*, Eur. Phys. J. **C66**, 215 (2010).

157. Supersymmetry Physics Results, ATLAS experiment, `http://twiki.cern.ch/twiki/bin/view/AtlasPublic/SupersymmetryPublicResults/`.

158. Supersymmetry Physics Results, CMS experiment, `http://cms-results.web.cern.ch/cms-results/public-results/publications/SUS/index.html`.